Study of Russian River Estuary Circulation and Water Quality

2011 Data Report

Report to
Sonoma County Water Agency (SCWA)

Prepared by

Matthew J. Robart & John L. Largier
Bodega Marine Laboratory (BML)
University of California Davis

Table of Contents

Acronyms & Terminology

ADCP	Acoustic Doppler Current Profiler
Anoxic	zero dissolved oxygen
BML	Bodega Marine Laboratory, University of California Davis
BOD	biochemical oxygen demand
BOON	Bodega Ocean Observing Node (www.bml.ucdavis.edu/boon)
CDIP	Coastal Data Information Program (cdip.ucsd.edu)
CTD	conductivity-temperature-depth profiling instrument
DO	dissolved oxygen
DWR	California Department of Water Resources
Halocline	level at which salinity changes rapidly with depth
Isothermal	no spatial difference in temperature
Isopycnal	no spatial difference in density, or line of equal density
NDBC	National Data Buoy Center (www.ndbc.noaa.gov)
NMFS	National Marine Fisheries Service (www.nmfs.noaa.gov)
PAR	photosynthetically active radiation
Pycnocline	level at which density changes rapidly with depth
ppt	parts per thousand (by mass)
PSU	practical salinity units
SBE	Seabird Electronics (www.seabird.com)
SCWA	Sonoma County Water Agency (www.scwa.ca.gov)
Thermocline	level at which temperature changes rapidly with depth

1. Introduction

This report summarizes data collected in the Russian River Estuary during the summer and fall of 2011 by Bodega Marine Laboratory (BML) personnel under contract from the Sonoma County Water Agency (SCWA). The purpose of this study was to elucidate patterns and mechanisms of water circulation and stratification within the estuary, with particular interest toward temperature, salinity, and dissolved oxygen (DO).

Data were collected during the months of May through November, which covers the portion of the year when river flow is seasonally lower. Low river flow is known to increase the probability of an extended closure of the estuary to the ocean by allowing ocean waves to build a sand bar across the estuary mouth. Separation from the ocean dramatically changes the physical forcing mechanisms in the estuary by removing or severely reducing the effect of tides as well as by preventing freshwater to flow out to the ocean. Both of these changes result in greater stratification within the estuary, which in turn can cause a reduction in dissolved oxygen at depth. The mouth exhibits a continuum of conditions from open (strongly tidal) to constricted (muted tides), perched (outflow only), and closed (zero surface flow, but seepage through sand bar may occur).

To monitor patterns of water flow, two Acoustic Doppler Current Profilers (ADCPs) were deployed. These instruments use acoustics to construct a vertical profile of current velocities throughout the water column at pre-set time intervals, and were strategically placed in deeper locations in the outer estuary (Patty's Rock) and in the inner estuary (Heron Rookery). Additionally, boat-based CTD surveys were conducted at a series of twelve sampling locations throughout the estuary on a regular basis. These surveys provided vertical profiles of salinity, temperature, DO, chlorophyll fluorescence, and turbidity at each station. The timing of the deployments and CTD surveys are summarized in Figure 1.1 and Table 1.1, and the approximate locations of the ADCP deployments and CTD stations are marked on the map in Figure 1.2.

To supplement these efforts, the following additional tasks were performed:

- Water level data loggers were used to measure water level and temperature at high temporal resolution in various sections of the estuary.
- Wind speed and direction were measured near the estuary mouth (at River's End Inn) and in the inner estuary (Freezeout Island) for a period of several weeks.

An extended closure of the estuary mouth was not observed during the study period, although reduced river flow allowed three brief closure events, increased stratification, and reduction in DO at some sampling stations, particularly in the inner estuary where tides have a reduced effect. The remainder of this report summarizes the data collected and provides some preliminary interpretations of the results.

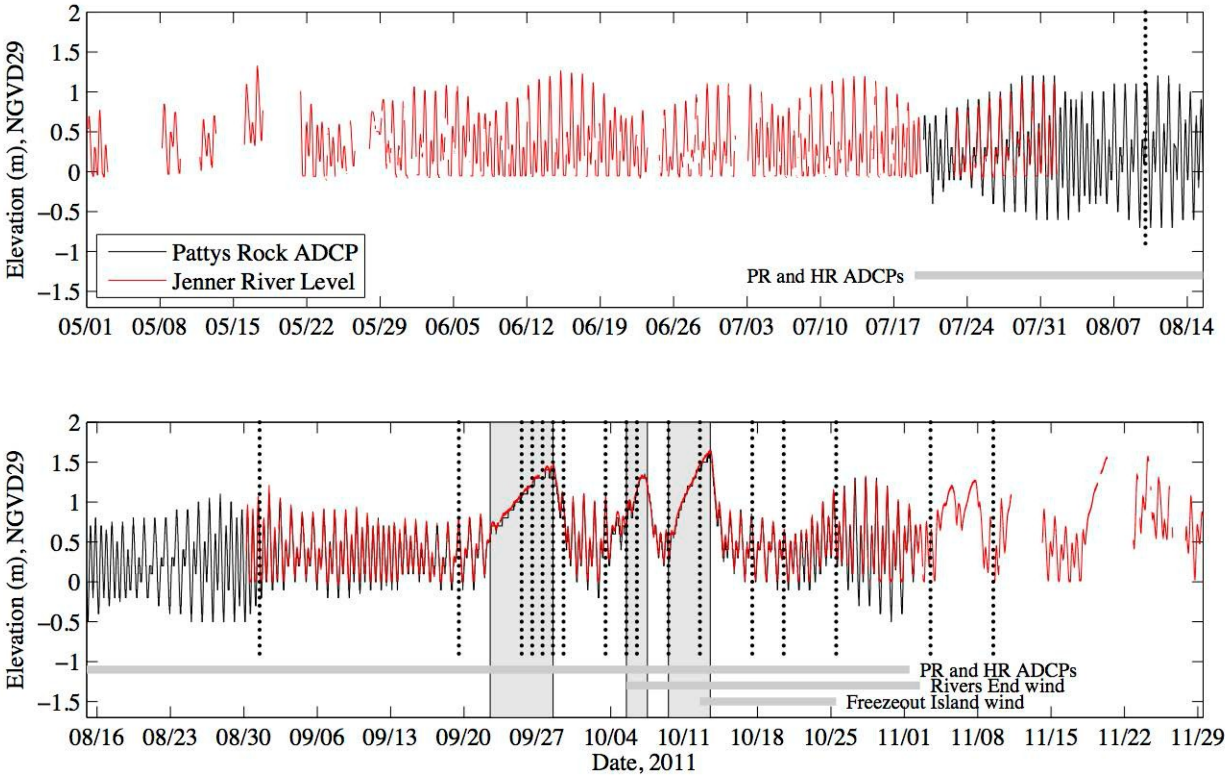

Figure 1.1 Timeline indicating water level at Jenner (red line) and the Patty's Rock ADCP (black line) during the 2011 study season. CTD transects are indicated by vertical dotted lines, and deployments of ADCPs at Patty's Rock (PR) and Heron Rookery (HR) as well as wind sensor deployments are indicated by horizontal gray lines. Closure periods are indicated by vertical gray bars.

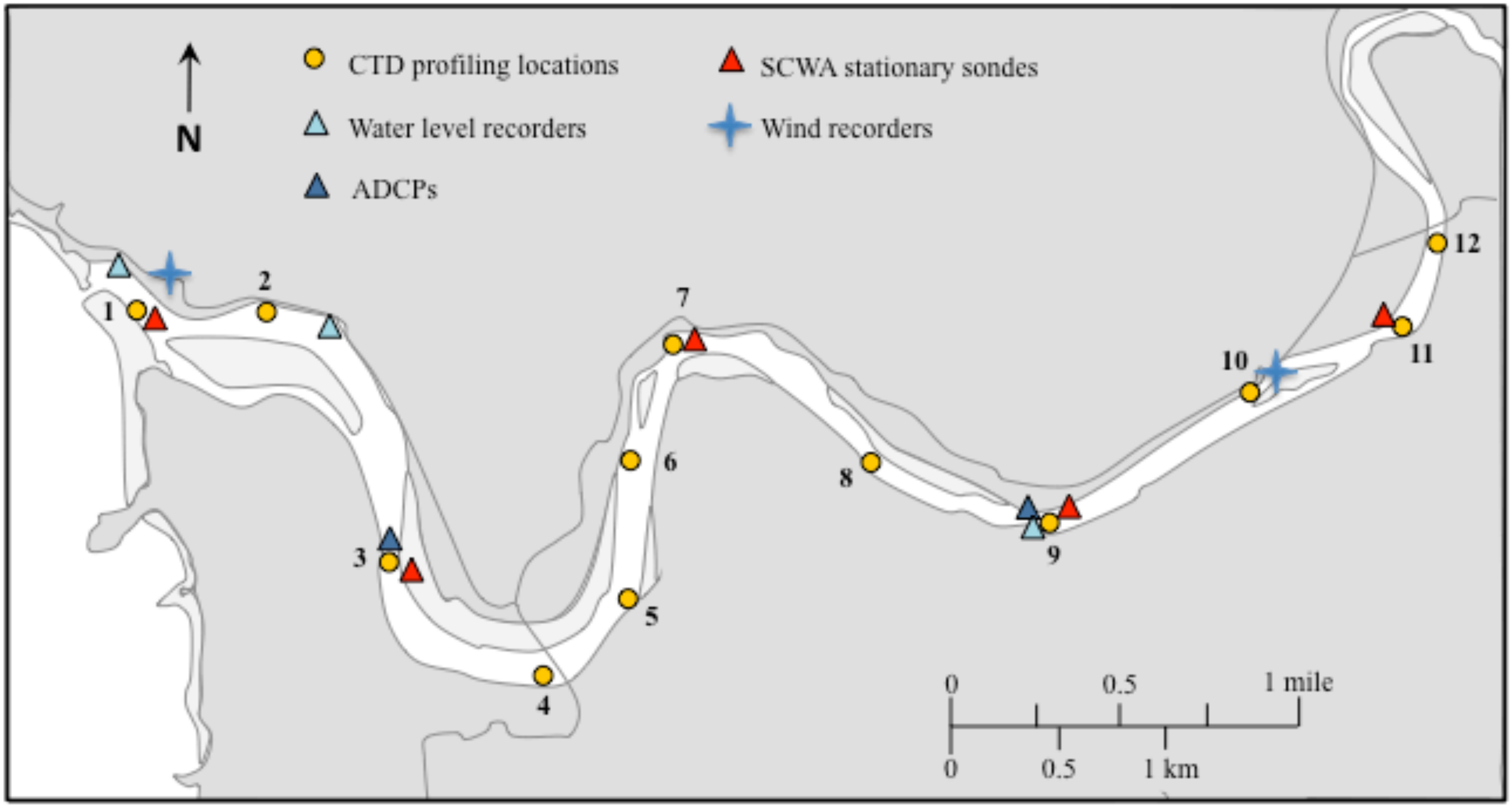

Figure 1.2 Map of the Russian River Estuary depicting the locations of data collection in 2011.

Table 1.1 Summary of data collection locations and dates.

Station No. (Fig 1.2)	Station Name	Data Collection	Approx. Location	Installation Date	Recovery Date
--	--	Temp/WL*	38.451339 N 123.127301 W	8/16/2011	10/31/2011
--	"River's End"	Wind		10/6/2011	11/3/2011
1	"Mouth"	CTD	38.449233 N 123.126348 W	--	--
2	"Penny Island"	CTD	38.450000 N 123.118519 W	--	--
3	"Patty's Rock"	CTD	38.439431 N 123.111656 W	--	--
		ADCP/WL*	38.439431 N 123.111656 W	7/19/2011	11/2/2011
4	"Bridgehaven"	CTD	38.434181 N 123.106194 W	--	--
5	"Willow Creek"	CTD	38.436320 N 123.098880 W	--	--
6	"Flats"	CTD	38.441228 N 123.098249 W	--	--
7	"Sheephouse Creek"	CTD	38.448496 N 123.095716 W	--	--
8	"Osprey Rookery"	CTD	38.444066 N 123.085145 W	--	--
9	"Heron Rookery"	CTD	38.440674 N 123.074972 W	--	--
		ADCP/WL*		7/19/2011	11/2/2011
		Temp/WL*		7/19/2011	8/18/2011
		Temp/WL*		9/20/2011	10/20/2011
10	"Freezeout Island"	CTD	38.446292 N 123.061210 W	--	--
		Wind		10/13/2011	10/26/2011
11	"Freezeout Creek"	CTD	38.449240 N 123.052573 W	--	--
12	"Moscow Bridge"	CTD	38.453700 N 123.049376 W	--	--

* WL: "water level," as determined from pressure sensor readings

2. Water Level Measurements

Two U20-model HOBO Water Level Loggers (Onset Computer, Inc.) were deployed in the estuary: at the mouth and at Heron Rookery. Water level was also recorded at the Jenner Visitor Center by the SCWA gauge and at Patty's Rock and Heron Rookery by the ADCPs. The HOBO loggers and Visitor Center gauge measured water level every two minutes, while the ADCPs sampled every ten minutes. These measurements served to allow examination of tides and wind seiches moving through the estuary as well as to provide a time series of water surface elevation in order to translate the instrument depth to actual elevations.

In order to convert pressure measured by the loggers into meaningful elevations, raw output was corrected for changes in atmospheric pressure using barometer data measured at Bodega Marine Laboratory as part of the Bodega Ocean Observing Node (BOON). Barometric pressure was measured at 30s intervals then averaged into 1-min data, which was then cleaned using a rate-of-change filter to remove points resulting in a rate of change greater than 0.5 mbar/min. Data points were matched in time, and barometric pressure was then subtracted from pressure measured by the instrument to obtain water pressure. Water pressure was converted to depth using density calculated using temperature measured by the logger and an assumed average salinity 16.5 PSU (error due to fluctuations in salinity and thermal stratification is less than 1%). To convert water depth to surface elevation, the instruments were corrected to match the SCWA gauge at Jenner between 2am and 8am (local time) on 25 September 2011, a time when winds were very light, the estuary mouth was closed, and flow into the estuary was low (~125 cfs). The error in the relative elevations is expected to be less than 2-3 cm.

Water levels also indicate periods when the estuary mouth is closed or perched. During these periods, the tidal signal is lost and the water level rises monotonically as freshwater is added to the estuary. Closure events were identified from photographic records, and three closure events are evident in the water level data from the 2011 study period: 22-29 September, 3-7 October, and 10-14 October (Figure 2.1). Water level can also indicate periods when the estuary mouth is notably constricted but not closed, which results in a muted tidal signal, i.e., low tides are higher than the ocean and high tides are lower than the ocean. This phenomenon often precedes a closure, and in 2011, muted tidal signals are evident during the month of September leading up to the full closure on 22 September (Figure 2.1).

Water level data also indicate the presence of a wind-driven seiche in the estuary. The sea breeze (see Section 6) pushes surface water landward, lowering water level near the mouth and raising water level in the inner estuary. The sloped water surface results in a pressure gradient that drives circulation within the estuary during closure events (Behrens, 2012). This phenomenon is observed during the first closure event of 2011, and is indicated by heightened water surface elevation at Heron Rookery compared with the mouth station each afternoon during the closure (Figure 2.2, green line). The subsequent two closure events of 2011 do not indicate the presence of this phenomenon (Figures 2.3 and 2.4), likely due to insufficient wind forcing (Figure 6.1).

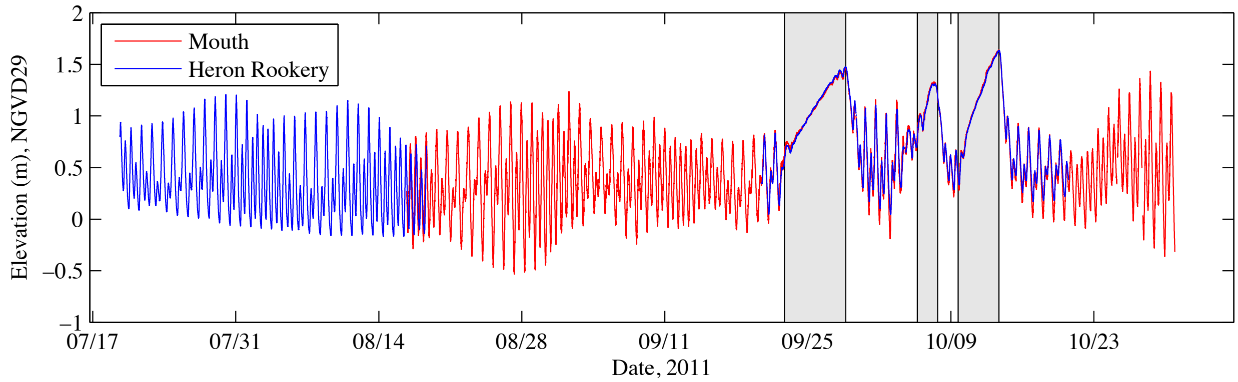

Figure 2.1 Water surface elevation derived from pressure readings taken at the mouth (red line) and at Heron Rookery (blue line). Gray bars indicate closure periods.

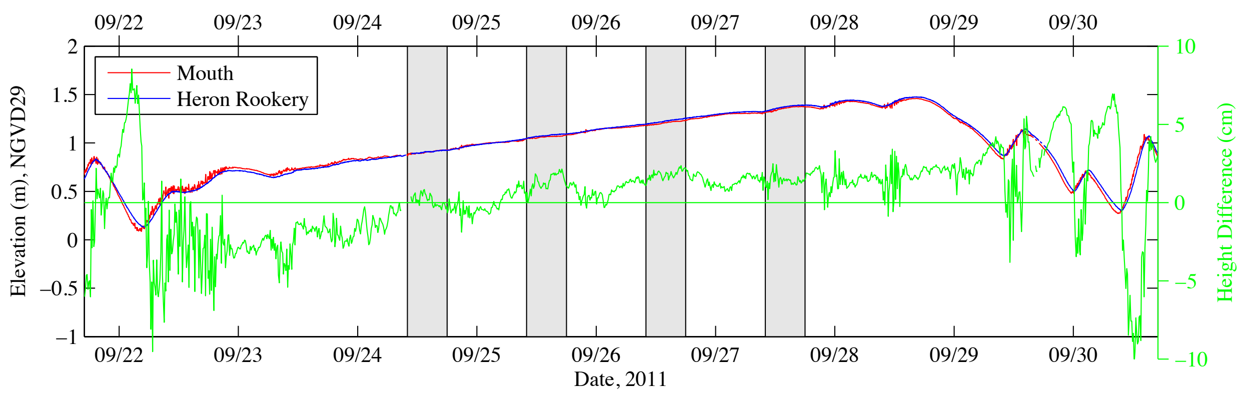

Figure 2.2 Water surface elevation derived from pressure readings taken at the mouth (red line) and at Heron Rookery (blue line) along with the difference between the two (green line) during the first closure event of 2011. Gray bars indicate the period of each day with the greatest landward wind (10am to 6pm local time). These time periods are associated with higher water surface elevation at Heron Rookery. X-axis ticks are centered on midnight local time.

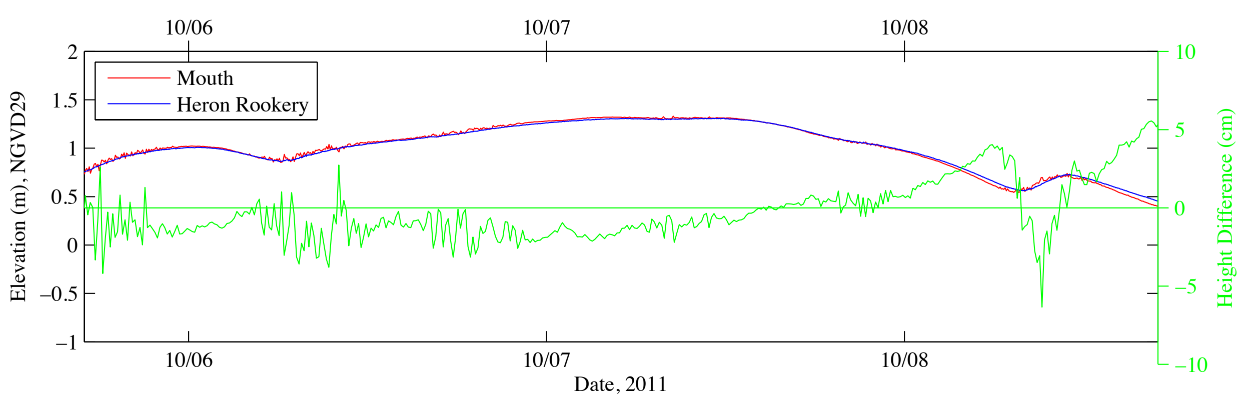

Figure 2.3 Water surface elevation derived from pressure readings taken at the mouth (red line) and at Heron Rookery (blue line) during the second closure event of 2011.

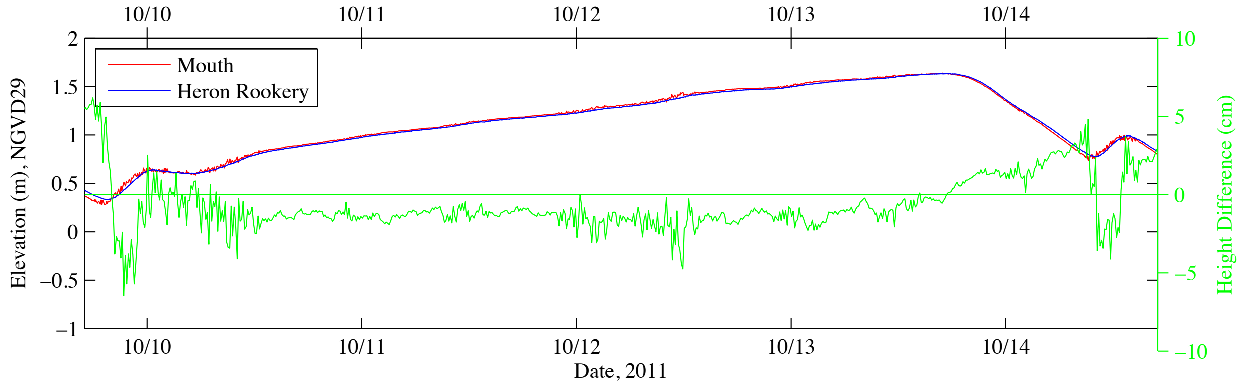

Figure 2.4 Water surface elevation derived from pressure readings taken at the mouth (red line) and at Heron Rookery (blue line) during the third closure event of 2011.

3. Biochemical Oxygen Demand

Biochemical oxygen demand (BOD) is a measure of the amount of oxidizable organic material present in water. More specifically, it is the amount of oxygen needed by aerobic microorganisms to break down all the organic material contained in a water sample. The procedure for determining BOD consists of taking a discrete bottle sample from the estuary, measuring the initial concentration of dissolved oxygen, then sealing and incubating the sample in the dark for a period of five days. After the incubation period, the concentration of oxygen is measured again, and the difference between the initial and final measures of oxygen is known as the 5-day BOD, which is a routine measure for the amount of organic material present in the sample.

Several attempts were made during the 2011 sampling season to take samples and determine accurate measures of BOD. However, each attempt failed at some point during the process, resulting in a lack of reliable BOD data for the entire study season. The first major problem involved air seeping into the samples during incubation. The glass bottles used for incubation have a glass stopper that must be sealed with a small volume of water around the rim, but low-humidity conditions in the incubator caused this reservoir to evaporate, allowing air into the sample. This problem was temporarily remedied by raising humidity in the incubator and rigorous manual refilling of the reservoir.

The other major problem with the 2011 BOD samples involved the probe used to measure oxygen concentration in the samples. Membrane-type oxygen probes are flow-rate-dependent, meaning that the measured concentration of oxygen increases as flow past the membrane increases because the membrane is encountering more oxygen molecules. The probe being used in 2011 required the user to maintain a constant stir rate in order to take an accurate sample, but after many attempts it was determined that the readings were not stable enough to produce reliable data.

During the off-season between the 2011 and 2012 field season, the BOD protocols were completely restructured in order to produce accurate and reliable data. The air seepage problem was remedied by the purchase of special caps that seal the small water reservoir, preventing evaporation during the incubation period. Furthermore, a new oxygen probe was purchased that is BOD-specific and includes a stirring system to standardize flow past the membrane. This has stabilized oxygen readings and with rigorous calibration and upkeep, this sensor is reliable and accurate to less than 1% of the reading.

4. Photographic Record of Mouth State

A StarDot SD500BN 5-megapixel camera was installed on 30 September 2011 near the estuary mouth on the Jenner Headlands property owned by the Sonoma Land Trust. This camera has a view of the estuary mouth, and takes a photograph hourly (plus one as a backup) between 8am and 6pm local time. In 2011, the camera took 1300 images over 86 days. These images serve as a record of the state of the mouth (open, constricted, perched, or closed) as well as the morphology of the beach and channel. Photographs are transmitted to a terminal at Goat Rock State Park then loaded to a database at Bodega Marine Laboratory where all photos are archived.

Figure 4.1 Sample image from the Russian River mouth camera. This image was taken on 07 October 2011 at 9:13am PDT and shows a small outlet channel along the jetty and evidence of wave overwash (swaths of darker sand to the right of the outlet channel).

5. Waves

Deep-water wave parameters were obtained from NDBC Buoy 46214 (cdip.ucsd.edu/?nav=historic&sub=data&stn=029&stream=p1), which is operated by the Coastal Data Information Program (CDIP) and is located approximately 62 km southwest of the estuary mouth. Deep-water waves differ from waves that make contact with the beach at the estuary mouth because refraction occurs as the waves shoal and interact with shelf bathymetry, but these data can still provide useful information about the regional wave climate leading up to closure events.

Wave data from the 2011 study period is provided in Figure 5.1. Several events are evident during this period when significant wave height reached approximately 4m. Each of the three brief mouth closure events during 2011 (22 September, 3 October, and 10 October) correspond with a wave event, but not all large wave events resulted in a mouth closure.

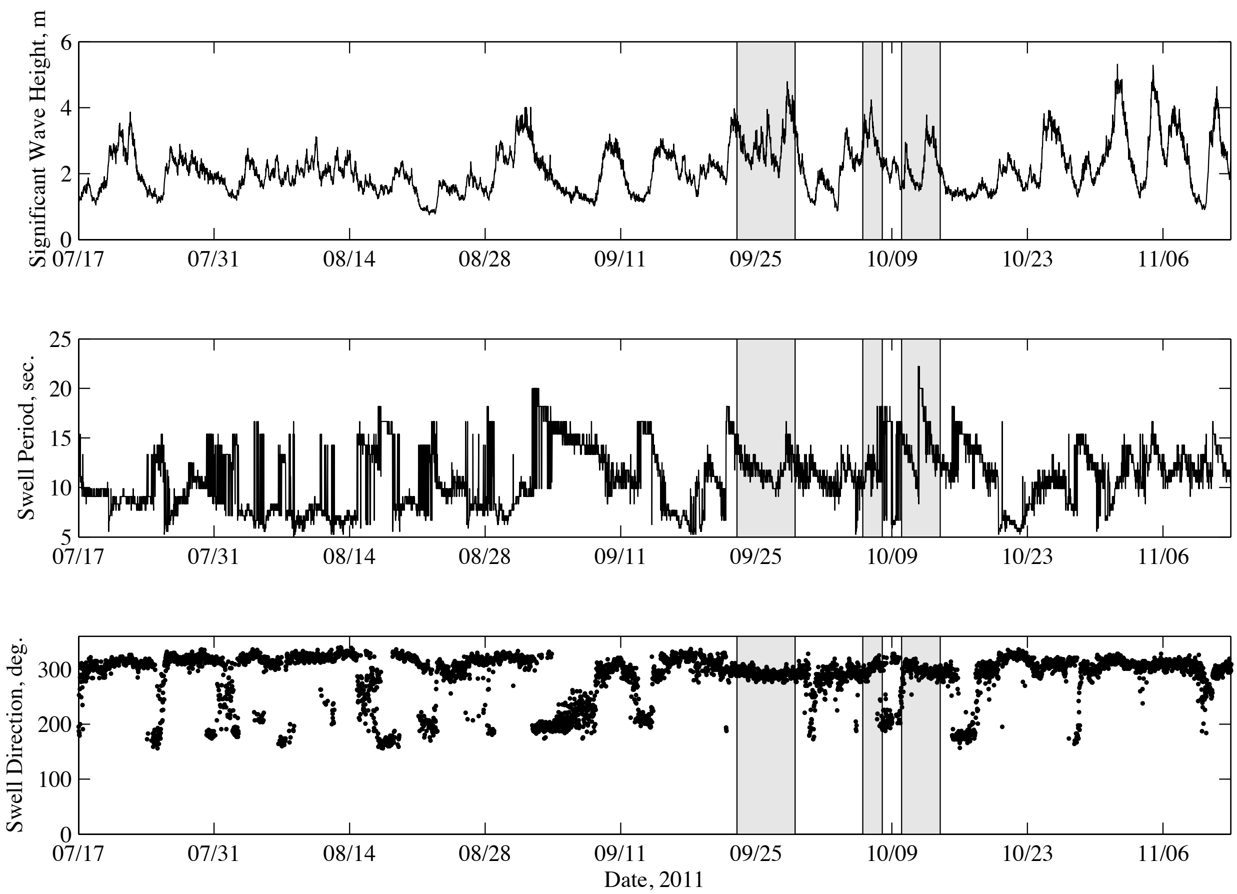

Figure 5.1 Significant wave height **(top)**, dominant swell period **(middle)**, and dominant swell direction **(bottom)** from NDBC buoy 46214. Gray bars indicate closure periods.

6. Wind

Two Davis anemometers were deployed in the estuary during the 2011 study season, with limited success. Problems with the sensors resulted in minimal wind data from two sites, one at River's End Restaurant & Inn near the mouth and the other at Freezeout Island in the inner estuary. The River's End station recorded valid data from 6 October until 3 November 2011, while the Freezeout Island station recorded data from 13 October until 26 October 2011.

Wind velocity (speed and direction) was decomposed into landward and cross-channel components for each site. In the case of the relatively long and narrow Russian River Estuary, the most relevant component of wind velocity is parallel to the channel (Figure 6.1)

The data from these sensors shows the presence of a diurnal sea breeze at both sites. Over the course of the time period when both sensors were operational (13-26 October 2011), the afternoon wind blowing in the landward direction was stronger at Freezeout Island than at River's End. Also, the "land breeze," or wind blowing toward the ocean at night, was more pronounced at the River's End site (Figure 6.1).

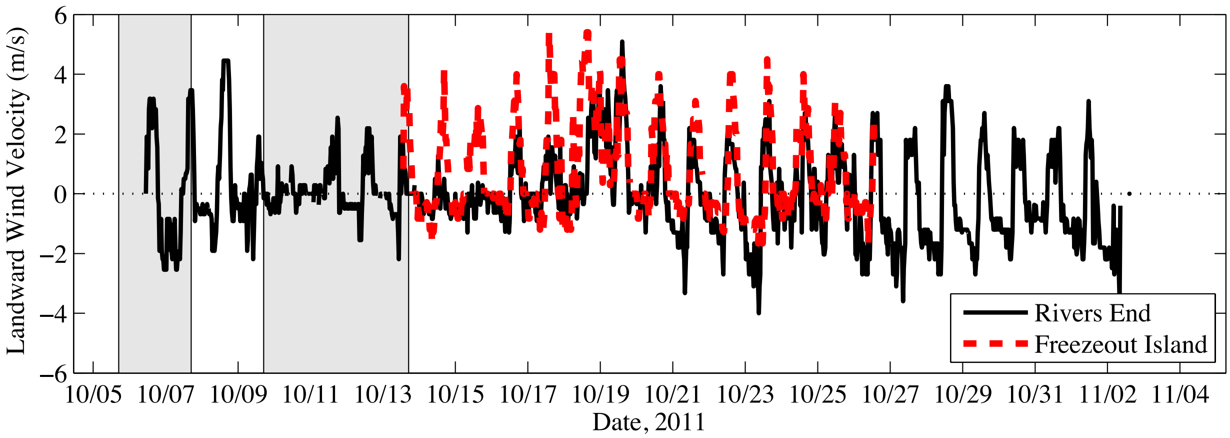

Figure 6.1 Landward component of wind velocity at River's End (solid black line) and Freezeout Island (dashed red line). Positive wind velocity indicates landward wind. Date ticks are centered at midnight local time and vertical gray bars indicate closure periods.

7. River Discharge

Measurements of Russian River discharge were obtained from the gauge operated by the U.S. Geological Survey (USGS) at Guerneville (station 11467000, waterdata.usgs.gov/nwis/). At the time of this report, these data are listed as provisional, subject to revision pending final approval. However, there are no known data quality issues during this time series.

River discharge remained above 100 cfs for the duration of the 2011 study season (Figure 7.1). Discharge stayed between 100 and 150 cfs for most of August and September, dropping to approximately 100 cfs just before the closure event that began on 23 September, but had increased again to 140 cfs by the time the mouth breached on 29 September. A rain event in early October caused a rise in discharge to over 400 cfs, but waves associated with this storm closed the mouth once again on 3 October. The mouth breached on 7 October, but closed following a drop in discharge to around 250 cfs on 10 October. This closure event ended on 14 October.

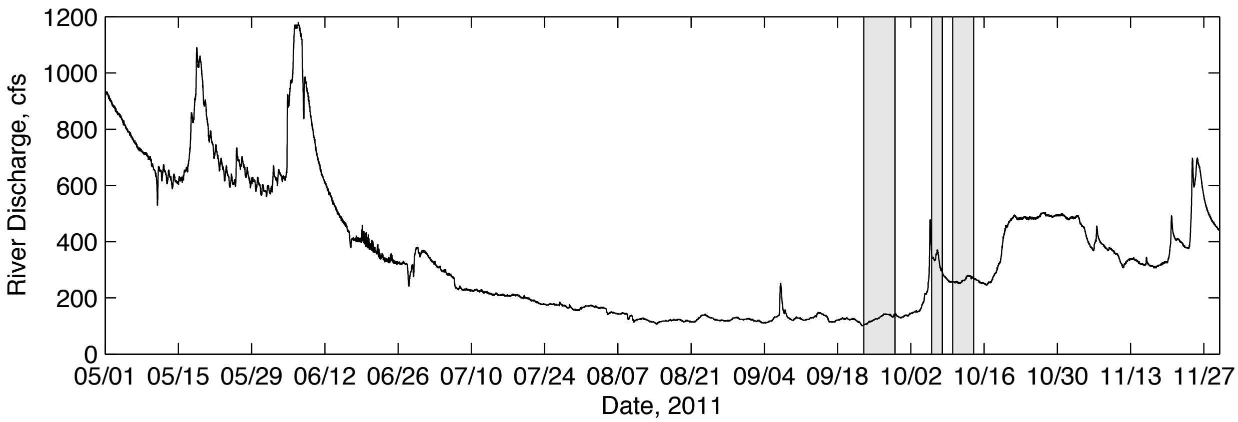

Figure 7.1 Russian River discharge measured at USGS gage 11467000 during the 2011 study period. Vertical gray bars indicate closure periods.

8. Channel Current Velocities

Two Acoustic Doppler Current Profilers (ADCPs) were deployed during the 2011 study period. One was deployed at Patty's Rock and the other was placed at Heron Rookery (Figure 1.1). Both instruments were sampling from 19 July through 2 November (Table 1.1). These locations were selected because they are both in deep pools, one in the outer estuary (Patty's Rock) and one in the inner estuary (Heron Rookery). The instruments measured and recorded a velocity profile of horizontal current velocity every 10 minutes with a vertical resolution of 0.5 m. Horizontal velocities are accurate to within ±0.3% of measured current, and in the case of the Russian River Estuary, velocity was not more than 1 m/s, resulting in an overall accuracy of <0.3 cm/s.

Current velocity (magnitude and direction) data were decomposed into along and cross-stream velocity components at each ADCP location. As with wind, the dominant component for current is parallel to the channel, which is reported here as a contour of all depths (Figures 8.1 and 8.2) as well as plots of velocity near the surface and the bottom at each location (Figure 8.3). The near-surface bin was determined using the pressure record from the ADCP to measure distance to the surface at each time point, then creating a new time series using the bin nearest to the surface (without breaking the surface itself) at each time point. The near-bottom bin was the first data bin above the ADCP, characterizing flow between 1.5m and 2m above the bottom.

At both locations, mean flows near the surface were toward the mouth while mean flows near the bottom were away from the mouth (Figure 8.3). This indicates an exchange of freshwater flowing out at the surface and saltwater flowing in at depth, as is typical of estuarine circulation. On a tidal scale, flows are toward the mouth during ebb tides and away from the mouth during flood tides at the surface at both locations. At Patty's Rock, landward flows up to 0.5 m/s are common near-bottom during spring flood tides (Figure 8.3). This indicates a strong influx of ocean water to the outer estuary when the mouth is open, especially during spring tides when the tidal range is large.

At Heron Rookery, flow near the bottom was generally very low, usually less than 0.1 m/s. However, several events were recorded when landward flow at the bottom exceeded 0.2 m/s during spring flood tides. Also, near the end of the study period bottom flow was observed to reach 0.4 m/s (Figure 8.3) toward the mouth during ebb tides when river discharge approached 500 cfs (Figure 7.1). This indicates that the enhanced river flow caused enough vertical mixing to remove the density stratification at this site, a process that took place over the course of approximately 14 days. This is evident in Figure 8.2 with negative velocities (toward the mouth) that gradually deepen from 15 October to 29 October 2011 at which point the entire water column appears to be moving in concert.

During the closure periods, flows were markedly reduced at both sites at the surface and the bottom. However, flow oscillations were still evident at the surface at Patty's Rock, and mean flows at the surface were toward the mouth, particularly at Heron Rookery.

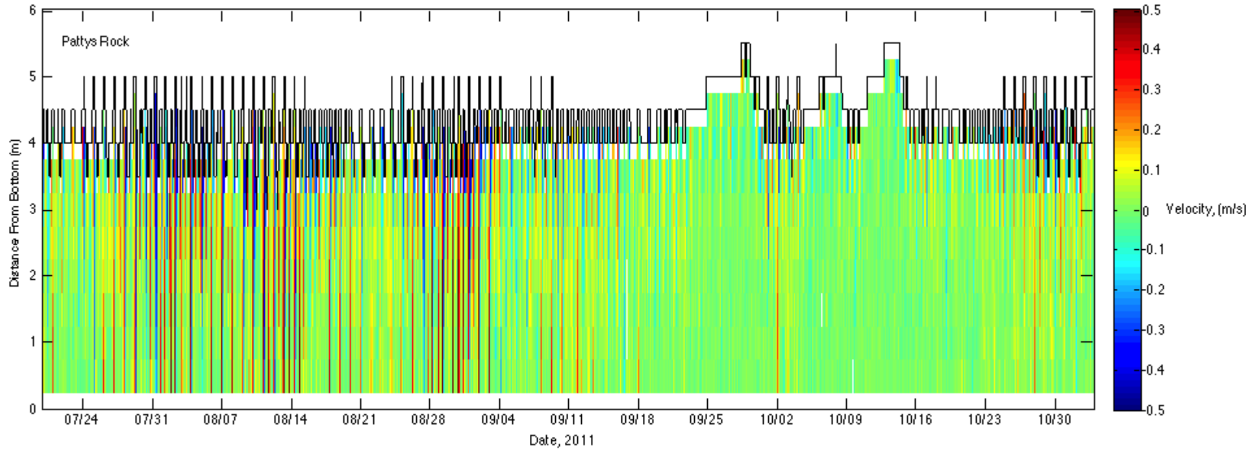

Figure 8.1 Contour plot of ADCP data collected at Patty's Rock. Negative flows are toward the mouth. Note the numerous landward flow events during periods when the estuary was tidal.

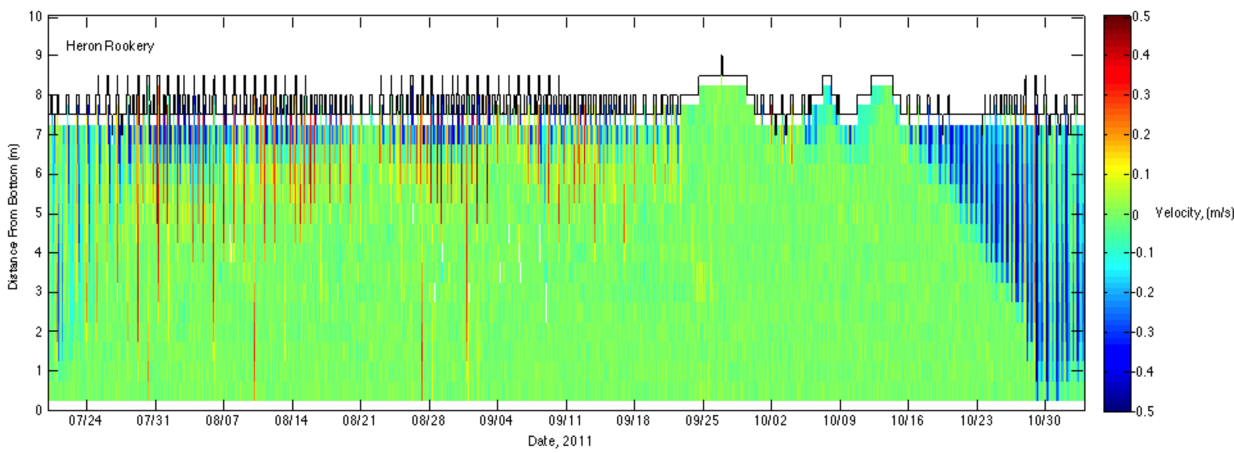

Figure 8.2 Contour plot of ADCP data collected at Heron Rookery. Negative flows are toward the mouth. Note that there are fewer landward flow events than at Patty's Rock, yet several strong flows can be seen in July and August. Also note the strong flows toward the mouth that extend progressively deeper into the water column at the end of the record.

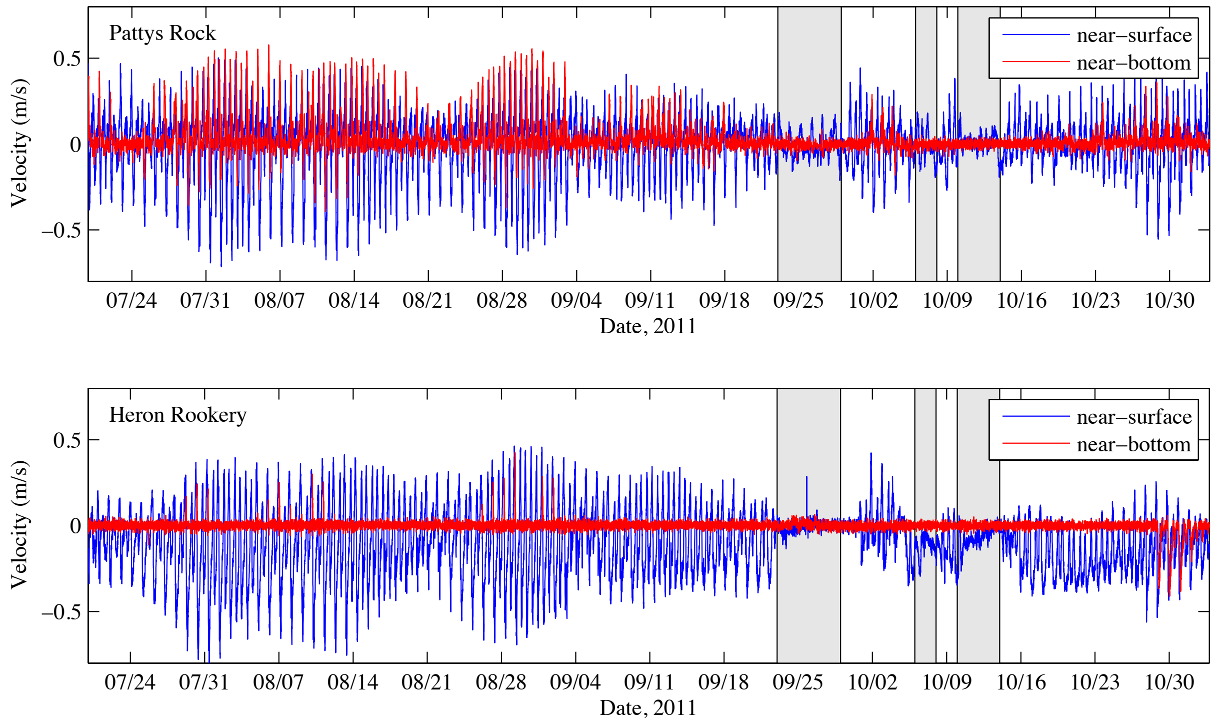

Figure 8.3 Near-surface (blue) and near-bottom (red) flow at Patty's Rock (top) and Heron Rookery (bottom) over the entire record. Negative flows are toward the mouth. Gray bars indicate closure periods.

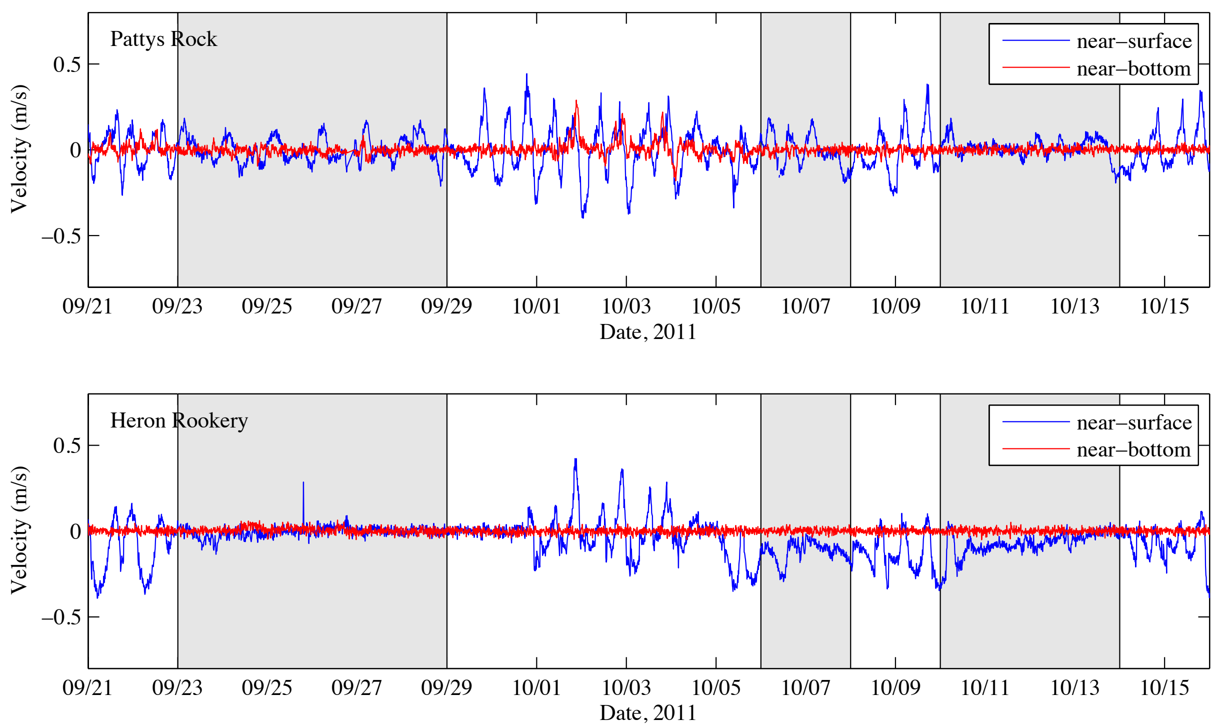

Figure 8.4 Near-surface (blue) and near-bottom (red) flow at Patty's Rock (top) and Heron Rookery (bottom) over the period from 21 September through 15 October. Negative flows are toward the mouth. Gray bars indicate closure periods.

9. CTD Transects

Contour plots were created based on spatial interpolation between CTD cast locations, which are represented by black dots on the plots. The elevations represented in the plots are based on water surface elevation at the time of each cast, and the interpolations were truncated at the thalweg depth based on distance from the mouth. The upper limit of the contouring was based on the uppermost data available in each cast and does not necessarily represent the elevation of the surface of the water.

The 10 August 2011 transect was conducted when the estuary mouth was open and flow within the estuary was strongly tidal. The most obvious spatial trend in the temperature and salinity data is the presence of warmer fresh water in the inner estuary and cooler salt water in the outer estuary. Some vertical stratification was present in the middle estuary but dissolved oxygen remained high throughout the water column at all stations. Chlorophyll fluorescence was low through much of the estuary, but a patch of chlorophyll was present in the middle estuary (Figure 9.1).

The 1 September 2011 transect was conducted when the estuary mouth was fully open and flow within the estuary was tidal. At this point, the inner estuary was still mainly comprised of warmer fresh water and the outer estuary was mostly cooler salt water. In fact, most of the stratification seen in the 10 August 2011 transect had disappeared, and dissolved oxygen remained high throughout the water column at all stations (Figure 9.2).

The 20 September 2011 transect was conducted three days before the first closure event of the season when the estuary mouth was beginning to constrict. Reduced tidal action produced increased salinity stratification and a drawdown of dissolved oxygen in the deep pools of the inner estuary (Figure 9.3).

The 26 September 2011 transect was conducted three days after the beginning of the first closure event. The salinity stratification and low-oxygen areas in the inner estuary had been washed out. This was due to the intrusion of high salinity water into the inner estuary that flushed out the deep pools with salty, but oxygen-rich water. Meanwhile, low oxygen areas were already developing at depth in the outer estuary by this time (Figure 9.4).

Two separate transects were conducted on 27 September 2011, four days after the beginning of the first closure event. By this time salinity was well stratified throughout the estuary except at the innermost stations. Dissolved oxygen remained low in the outer estuary and relatively high at the inner estuary stations. Chlorophyll fluorescence was low in the upper water column with patches of high chlorophyll near the bottom throughout the estuary. The beam transmission data shows a layer of very turbid water at the halocline (Figure 9.5 and 9.6), indicating that sunlight was likely prohibited from reaching the lower layers of water, which can contribute to oxygen drawdown.

On 28 September 2011, temperature and salinity patters were similar to those seen on the previous day, and chlorophyll remained highest in the lower sections of the water column, particularly in the outer estuary. Dissolved oxygen data from this transect show a midwater layer of supersaturation, likely due to oxygen produced by phytoplankton photosynthesis. DO was still very low at the bottom in the outer estuary, and the deep pools in the middle to inner estuary also showed signs of oxygen depletion (Figure 9.7).

The transect on 29 September 2011 was conducted just before the sand berm at the mouth was breached. Temperature and salinity data appeared very similar to the previous two days, and DO also showed a similar pattern to the previous transect although oxygen was drawn down slightly farther in the deep pools of the middle to inner estuary. Chlorophyll fluorescence was highest in the outer estuary throughout the water column (Figure 9.8).

The 30 September 2011 transect was conducted one day after the estuary mouth opened, and the change in conditions is reflected in the temperature and salinity data. Compared with the previous day, the wedge of cooler salty water had been pushed back toward the ocean by approximately 1 km. However, DO conditions in the bottom layer remained low throughout much of the estuary except within 1.5 km of the mouth where oxygen-rich ocean water had been brought in with the incoming tide. It appears as though the breach had still not created enough circulation to mix or transport the salt water that had been trapped in the deep pools during the closure event. Chlorophyll fluorescence remained highest in the outer estuary, and a patch of high chlorophyll water had extended farther landward near the surface (Figure 9.9).

By 4 October 2011, the estuary mouth had been open for five days, and temperature and salinity conditions appeared very similar to what was seen on the 30 September transect four days earlier. However, the DO patterns in the estuary were very different. The oxygen levels in the bottom layer of the outer estuary were much higher than previously found, but oxygen was severely depleted at Sheephouse Creek and Heron Rookery, thus confirming that bottom water in those pools had remained trapped since it intruded prior to 26 September. Chlorophyll fluorescence was low though most of the estuary, but levels remained high very near the mouth (Figure 9.10).

On 6 October 2011 the estuary mouth had closed once again, although conditions were very different from those seen at the beginning of the first closure. The salt wedge had not pushed landward, likely because river discharge was significantly higher than it had been at the beginning of the first closure (Figure 7.1). Anoxic water persisted in deep pools at Sheephouse Creek and Heron Rookery, plus a new hypoxic water mass had developed near the mouth. Chlorophyll fluorescence was very low throughout most of the estuary (Figure 9.11).

Conditions during the 7 October 2011 transect were very similar to those seen on the previous day, although oxygen depletion was seen throughout a larger portion of the outer estuary. Also, a subsurface chlorophyll fluorescence maximum was seen in the middle and outer estuary (Figure 9.12).

By the time the next transect was conducted on 10 October 2011, the estuary mouth had opened and then closed once again. Temperature and salinity patterns appeared very similar to those seen during the previous closure, on 6 and 7 October (Figures 9.11, 9.12). DO, however, was more severely depleted and throughout a more extensive portion of the estuary. With the outflow of the surface layer and drop in water level, this DO-depleted layer filled much of the water column in the middle and outer estuary. Also, chlorophyll levels were low throughout most of the estuary except very high levels were seen near the surface in the middle and outer estuary (Figure 9.13). Judging from the absence of bottom currents (Figures 8.2 and 8.3), the lower layer was not flushed out during the breach on 8 October and anoxic conditions persisted.

The transect conducted on 13 October 2011 came three days after the mouth closed. Salinity was vertically stratified throughout most of the estuary with a lens of fresh water at the surface that was approximately 1 - 1.5 m deep. Chlorophyll fluorescence was low through most of the estuary, but a patch of higher chlorophyll water was seen in the outer estuary. DO levels were low through most of the bottom layer, although the pattern appeared more patchy than in the previous transect (Figure 9.14).

On 18 October 2011, the estuary mouth had been open for four days and the river was discharging over 250 cfs (Figure 7.1). This caused the bulk of the salt water to be pushed toward the ocean, but salinity stratification was still prevalent at Heron Rookery, Osprey Rookery, and Sheephouse Creek. Furthermore, DO at these stations and throughout the middle estuary was still very low, indicating that the enhanced river flow was still not enough to remove the high-salinity water in the deep pools (Figure 9.15 see also ADCP velocities, Figure 8.3).

By 21 October 2011, river discharge had to increased to over 450 cfs (Figure 7.1), causing the salt to be pushed further toward the ocean. This resulted in a deepening of the surface layer and reduction of salinity in the bottom layer at Heron Rookery, indicating that the enhanced flow was causing a significant increase in vertical mixing at this station. Furthermore, DO had increased to non-hypoxic levels. At Osprey Rookery, the salt had been totally removed and DO was back to normal levels. However, salinity was still stratified from Sheephouse Creek to Bridgehaven, and DO remained very low in the bottom layer at these stations indicating that this deep water had been retained since the closure period a week earlier. Chlorophyll fluorescence was patchy, with high chlorophyll levels near the halocline in the middle and outer estuary (Figure 9.16).

The data from the 26 October 2011 transect shows that the salt had been pushed even farther downstream, although deep pockets of salty, low DO water remained at Heron Rookery and Sheephouse Creek (Figure 9.17). By 4 November 2011, nearly all the saltwater had been removed from Heron Rookery and only slightly oxygen-depleted water was found near the bottom there. Much of the saltwater had also been removed from the Sheephouse Creek station, yet DO was still very low in the deepest section. High chlorophyll water was found below the surface in the middle estuary on both 26 October and 4 November, near the leading edge of the salt wedge (Figures 9.17 and 9.18).

Five separate transects were conducted on 10 November 2011 in order to investigate how water moves through the estuary on a tidal cycle. By this time, river discharge had dropped back to near 300 cfs (Figure 7.1), allowing saltwater to migrate farther upstream once again. This led to salinity stratification and oxygen drawdown at the Heron Rookery and Sheephouse Creek stations. Chlorophyll fluorescence was variable throughout the day, but a patch of high chlorophyll water was present in the middle estuary during all five transects (Figures 9.19, 9.20, 9.21, 9.22, and 9.23).

Table 9.1 Dates, times, and parameters sampled during each CTD transect of 2011.

CTD Transects			Parameters Sampled						
Date	**Start (local)**	**End (local)**	**T**	**S**	**Fl**	**DO**	**BT**	**PAR**	**pH**
10-Aug-2011	10:47	14:04	•	•	•	•	•	•	
1-Sep-2011	11:49	15:17	•	•		•			•
20-Sep-2011	9:58	12:10	•	•		•			•
26-Sep-2011	9:54	11:32	•	•		•			•
27-Sep-2011 "A"	9:29	10:36	•	•	•	•	•		
27-Sep-2011 "B"	11:22	12:26	•	•	•	•	•		
28-Sep-2011	9:13	10:14	•	•	•	•	•		
29-Sep-2011	15:44	16:45	•	•	•	•	•		
30-Sep-2011	15:59	16:45	•	•	•	•	•		
4-Oct-2011	11:33	13:27	•	•	•	•	•		
6-Oct-2011	10:50	11:38	•	•	•	•	•		
7-Oct-2011	10:03	10:47	•	•	•	•	•		
10-Oct-2011	11:27	12:09	•	•	•	•	•		
13-Oct-2011	12:16	13:02	•	•	•	•	•		
18-Oct-2011	12:10	13:24	•	•	•	•	•		
21-Oct-2011	9:35	10:38	•	•	•	•	•		
26-Oct-2011	12:41	13:26	•	•	•	•	•		
4-Nov-2011	9:32	10:22	•	•	•	•	•		
10-Nov-2011 "A"	8:26	9:18	•	•	•	•	•		
10-Nov-2011 "B"	9:46	10:32	•	•	•	•	•		
10-Nov-2011 "C"	11:19	12:06	•	•	•	•	•		
10-Nov-2011 "D"	12:50	13:36	•	•	•	•	•		
10-Nov-2011 "E"	14:35	15:17	•	•	•	•	•		

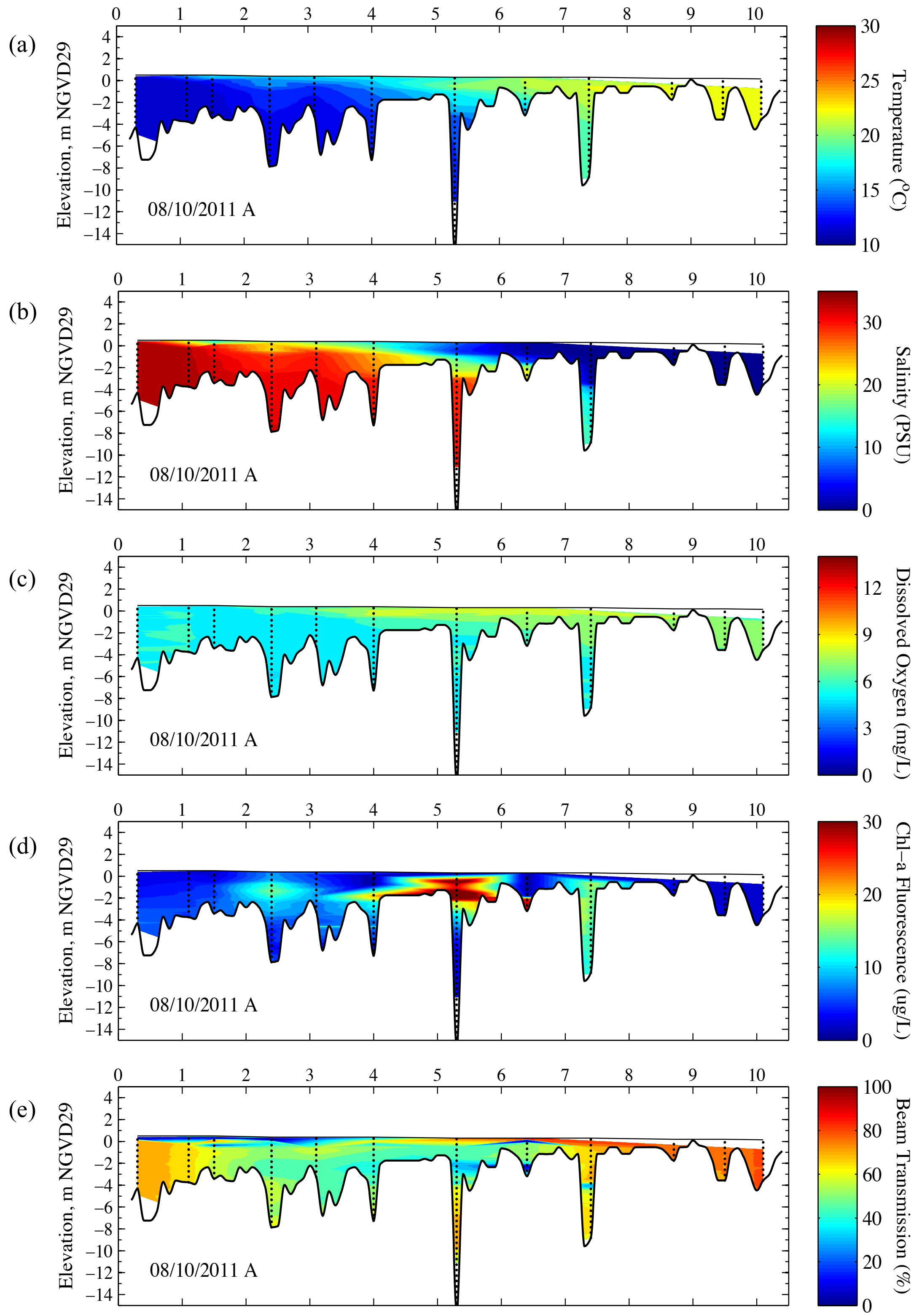

Figure 9.1 Contours of temperature (a), salinity (b), dissolved oxygen (c), chlorophyll fluorescence (d), and beam transmission (e) collected on 10 August 2011. The x-axis represents distance (in km) from the estuary mouth.

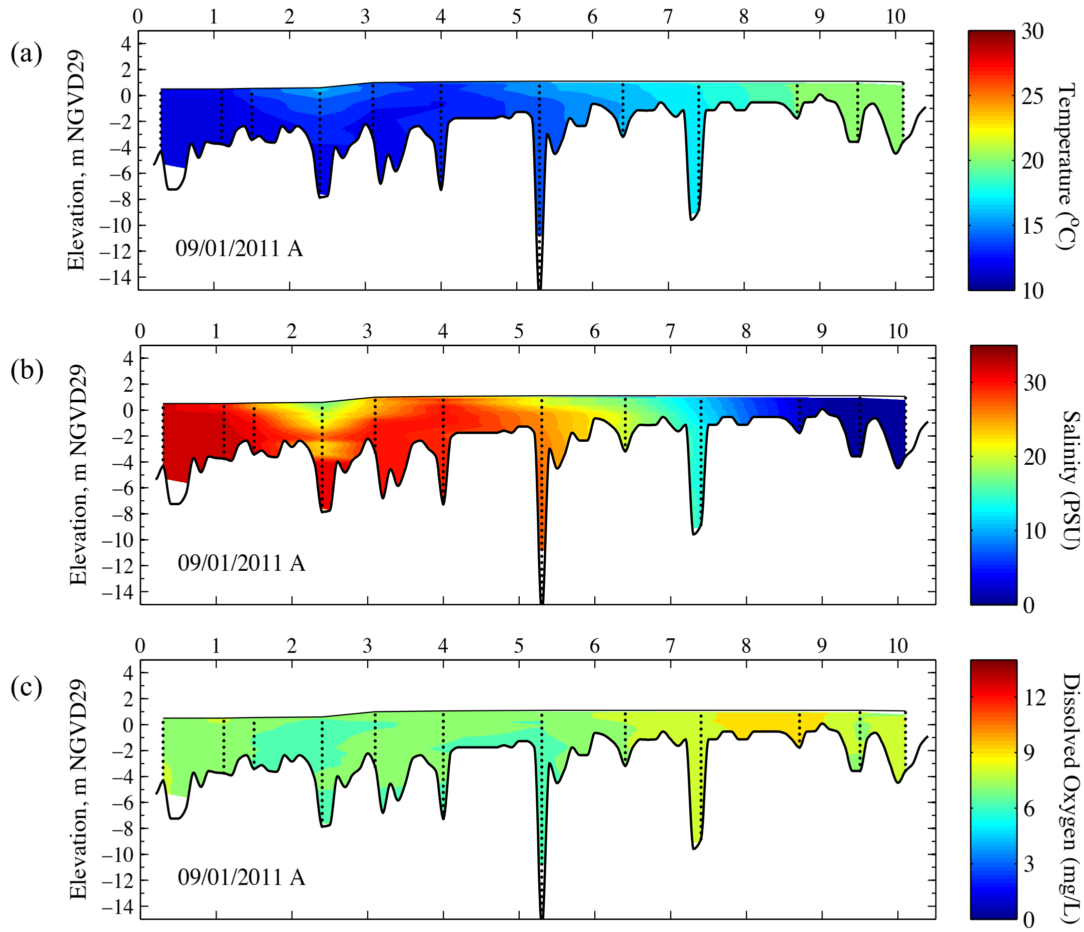

Figure 9.2 Contours of temperature (a), salinity (b), and dissolved oxygen (c) collected on 1 September 2011. The x-axis represents distance (in km) from the estuary mouth.

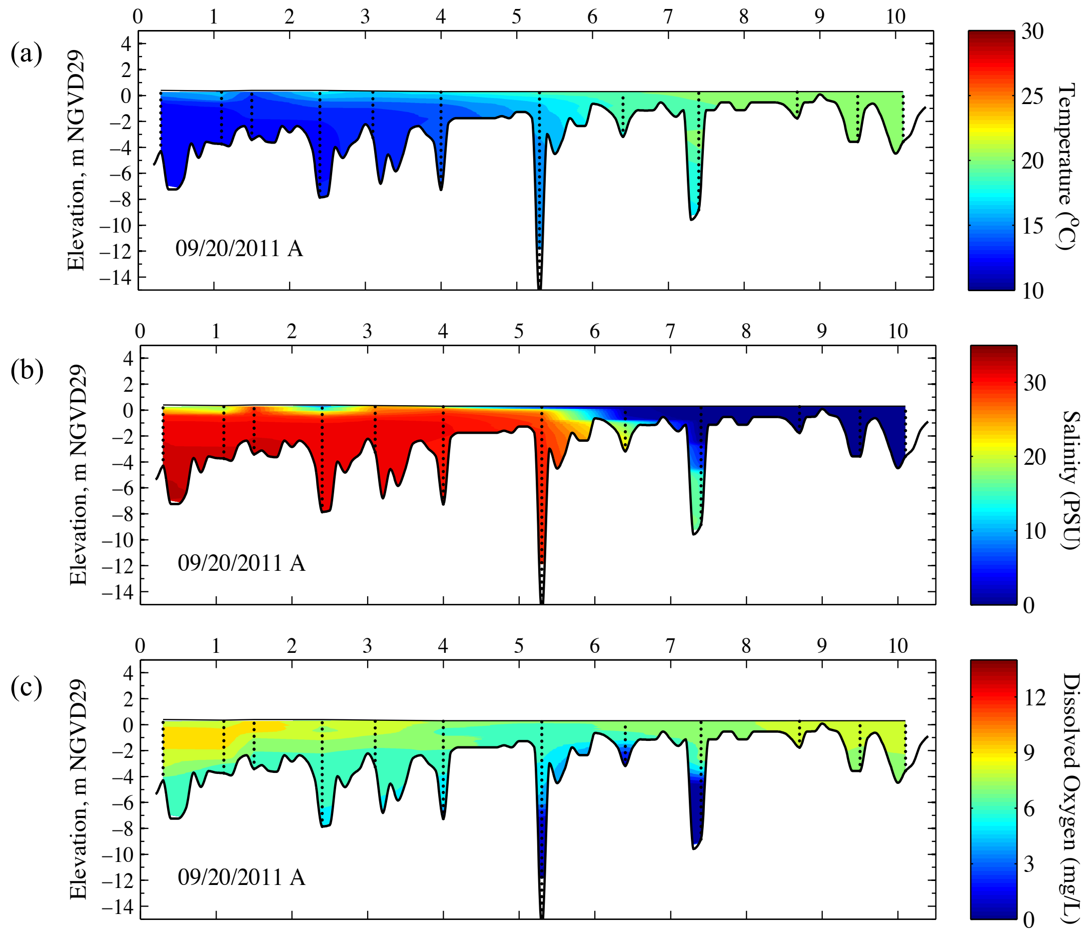

Figure 9.3 Contours of temperature (a), salinity (b), and dissolved oxygen (c) collected on 20 September 2011. The x-axis represents distance (in km) from the estuary mouth.

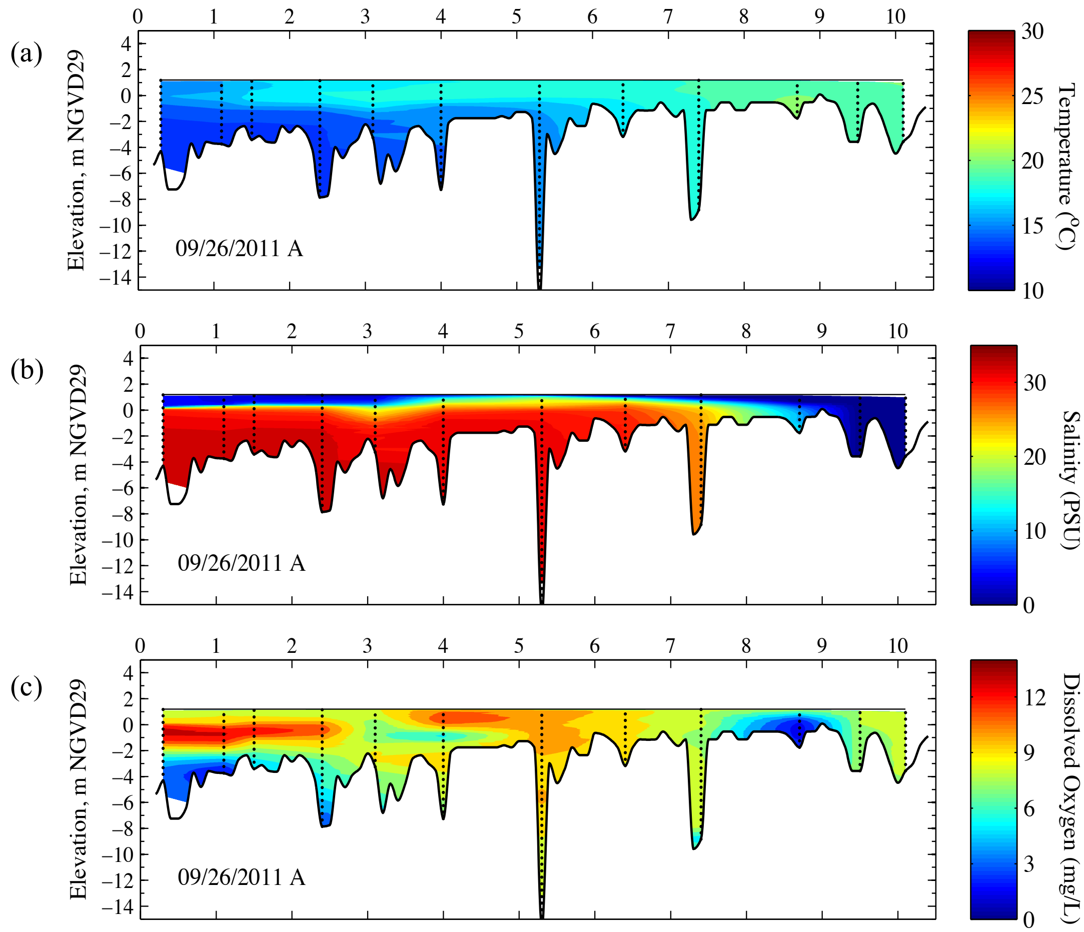

Figure 9.4 Contours of temperature (a), salinity (b), and dissolved oxygen (c) collected on 26 September 2011. The x-axis represents distance (in km) from the estuary mouth.

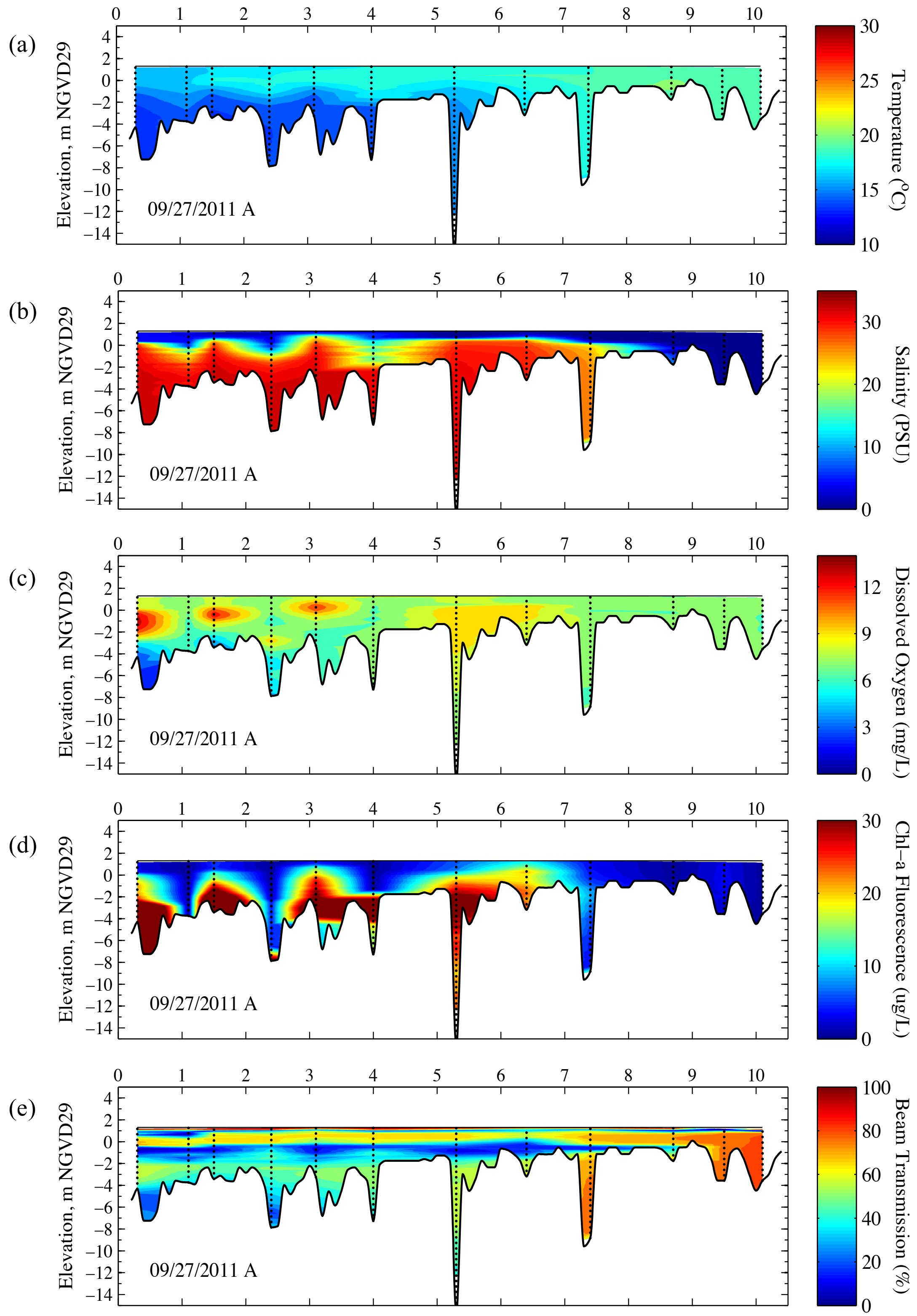

Figure 9.5 Contours of temperature (a), salinity (b), dissolved oxygen (c), chlorophyll fluorescence (d), and beam transmission (e) collected during the first transect on 27 September 2011. The x-axis represents distance (in km) from the estuary mouth.

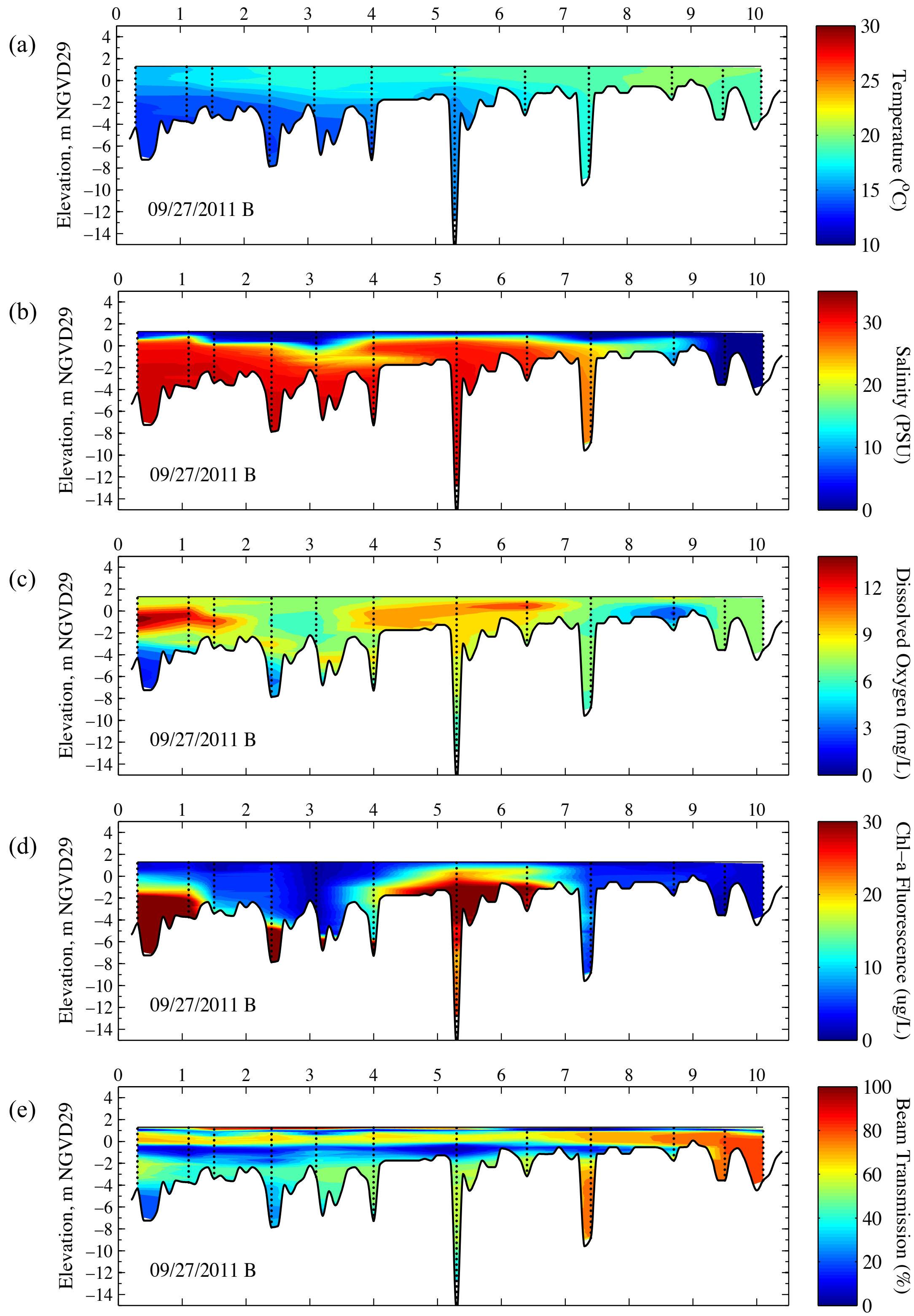

Figure 9.6 Contours of temperature (a), salinity (b), dissolved oxygen (c), chlorophyll fluorescence (d), and beam transmission (e) collected during the second transect on 27 September 2011. The x-axis represents distance (in km) from the estuary mouth.

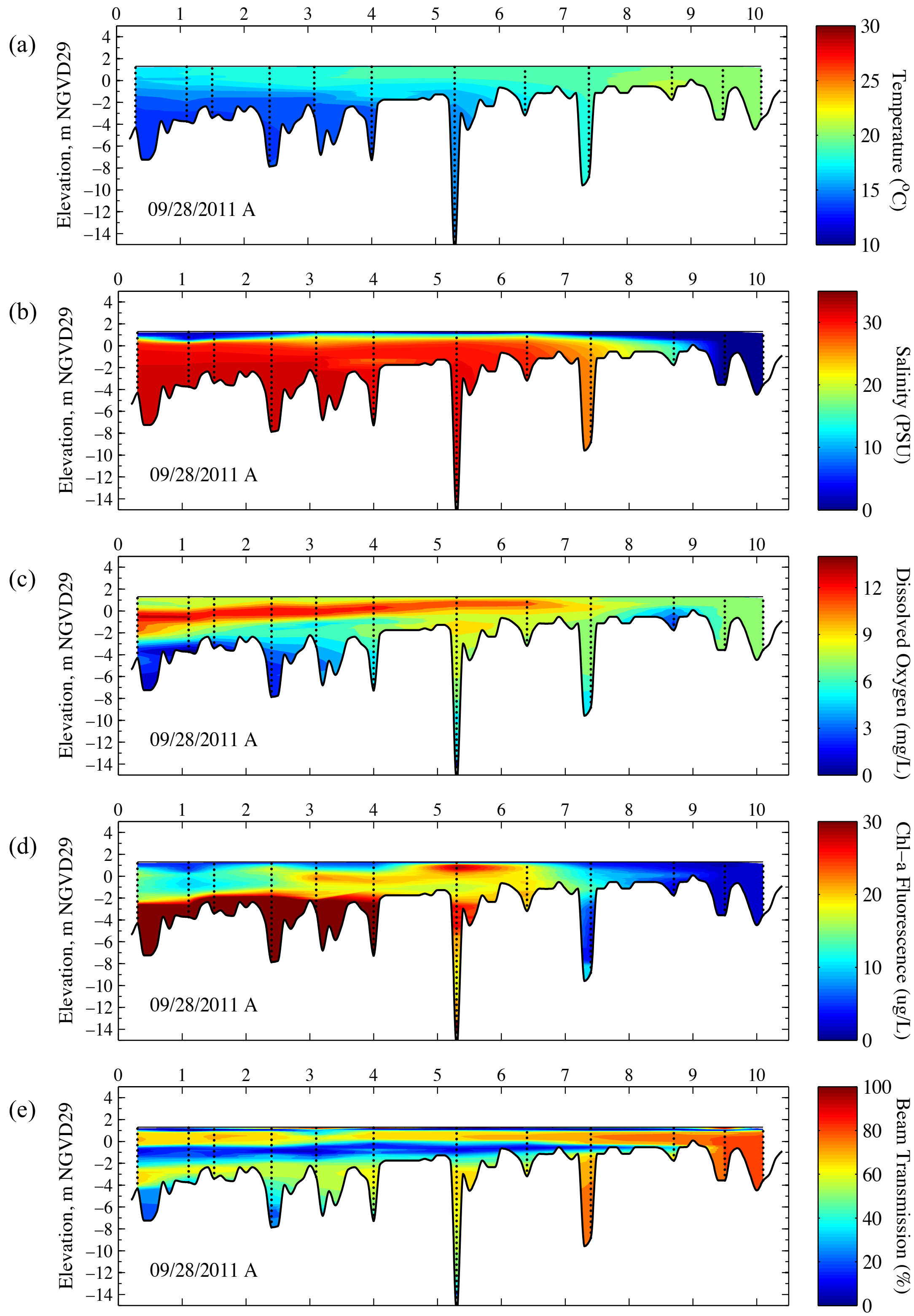

Figure 9.7 Contours of temperature (a), salinity (b), dissolved oxygen (c), chlorophyll fluorescence (d), and beam transmission (e) collected on 28 September 2011. The x-axis represents distance (in km) from the estuary mouth.

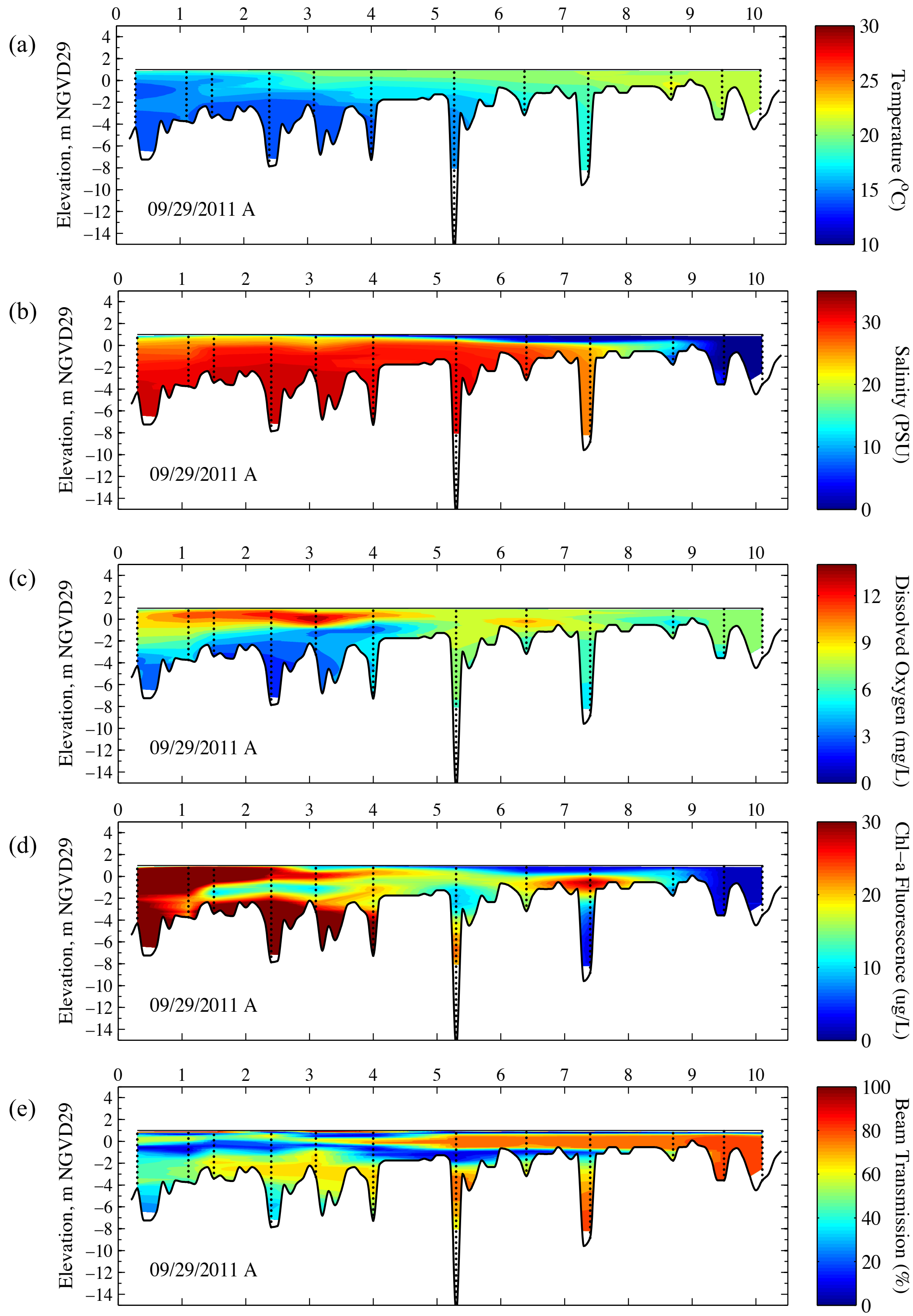

Figure 9.8 Contours of temperature (a), salinity (b), dissolved oxygen (c), chlorophyll fluorescence (d), and beam transmission (e) collected on 29 September 2011. The x-axis represents distance (in km) from the estuary mouth.

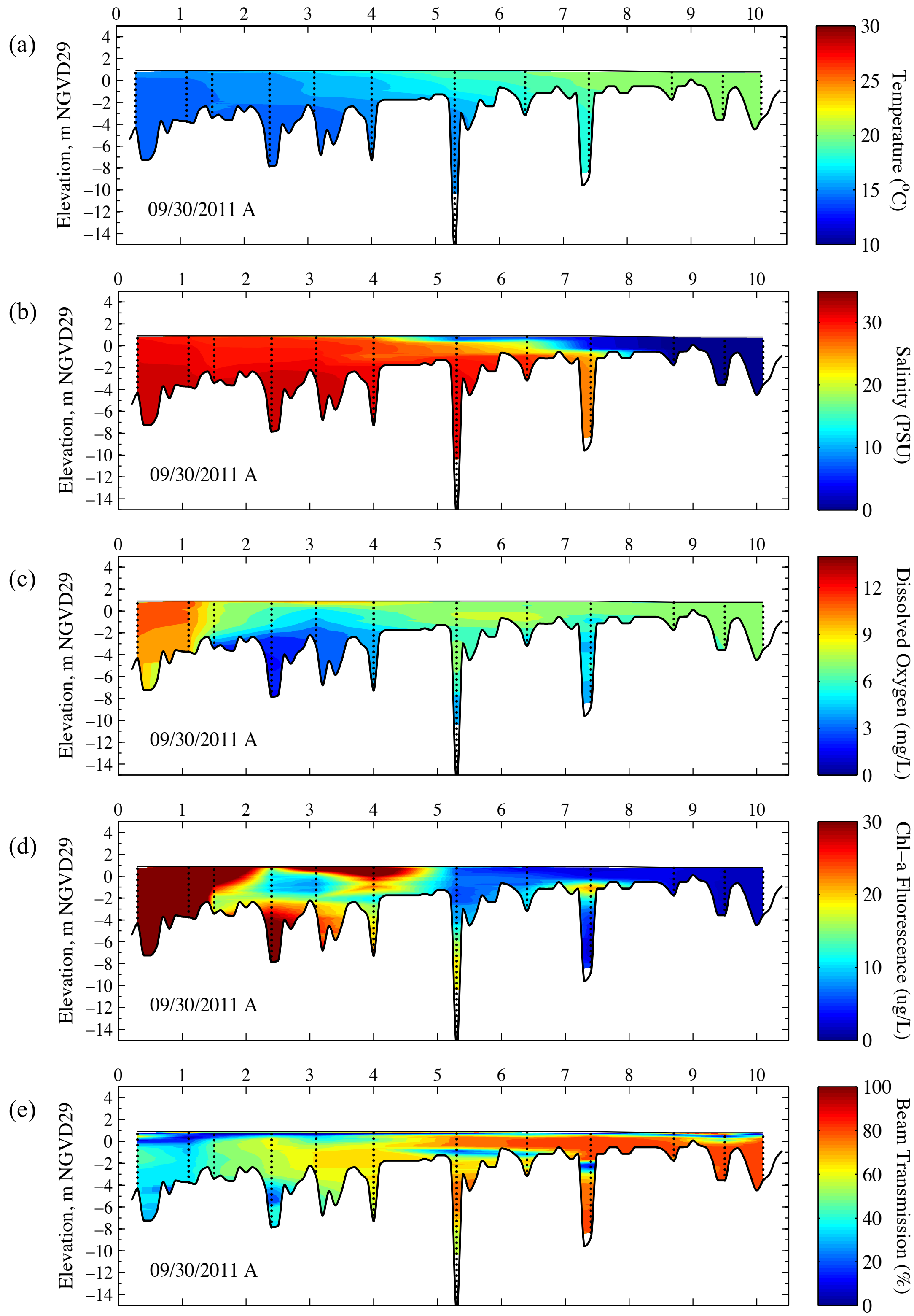

Figure 9.9 Contours of temperature (a), salinity (b), dissolved oxygen (c), chlorophyll fluorescence (d), and beam transmission (e) collected on 30 September 2011. The x-axis represents distance (in km) from the estuary mouth.

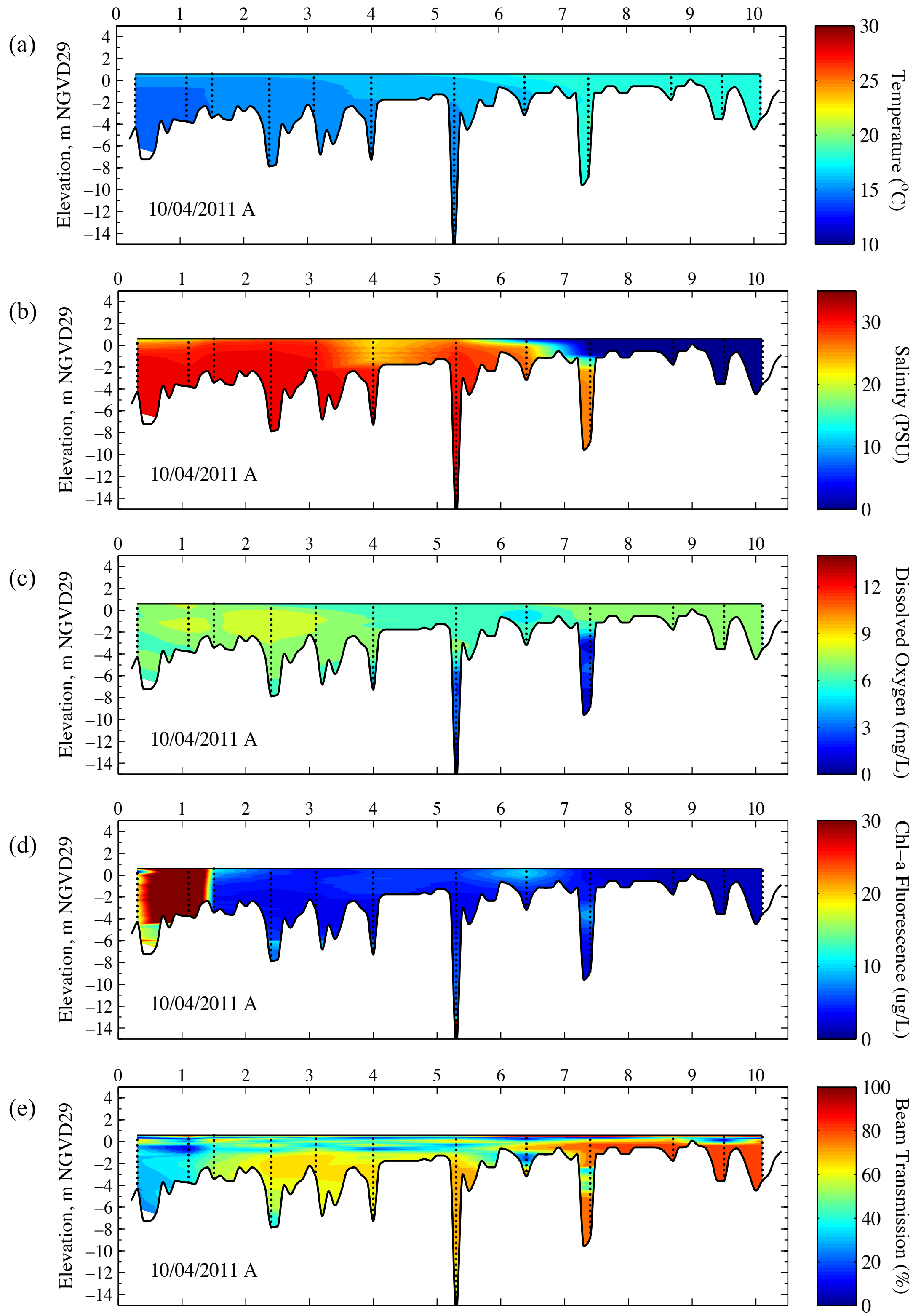

Figure 9.10 Contours of temperature (a), salinity (b), dissolved oxygen (c), chlorophyll fluorescence (d), and beam transmission (e) collected on 4 October 2011. The x-axis represents distance (in km) from the estuary mouth.

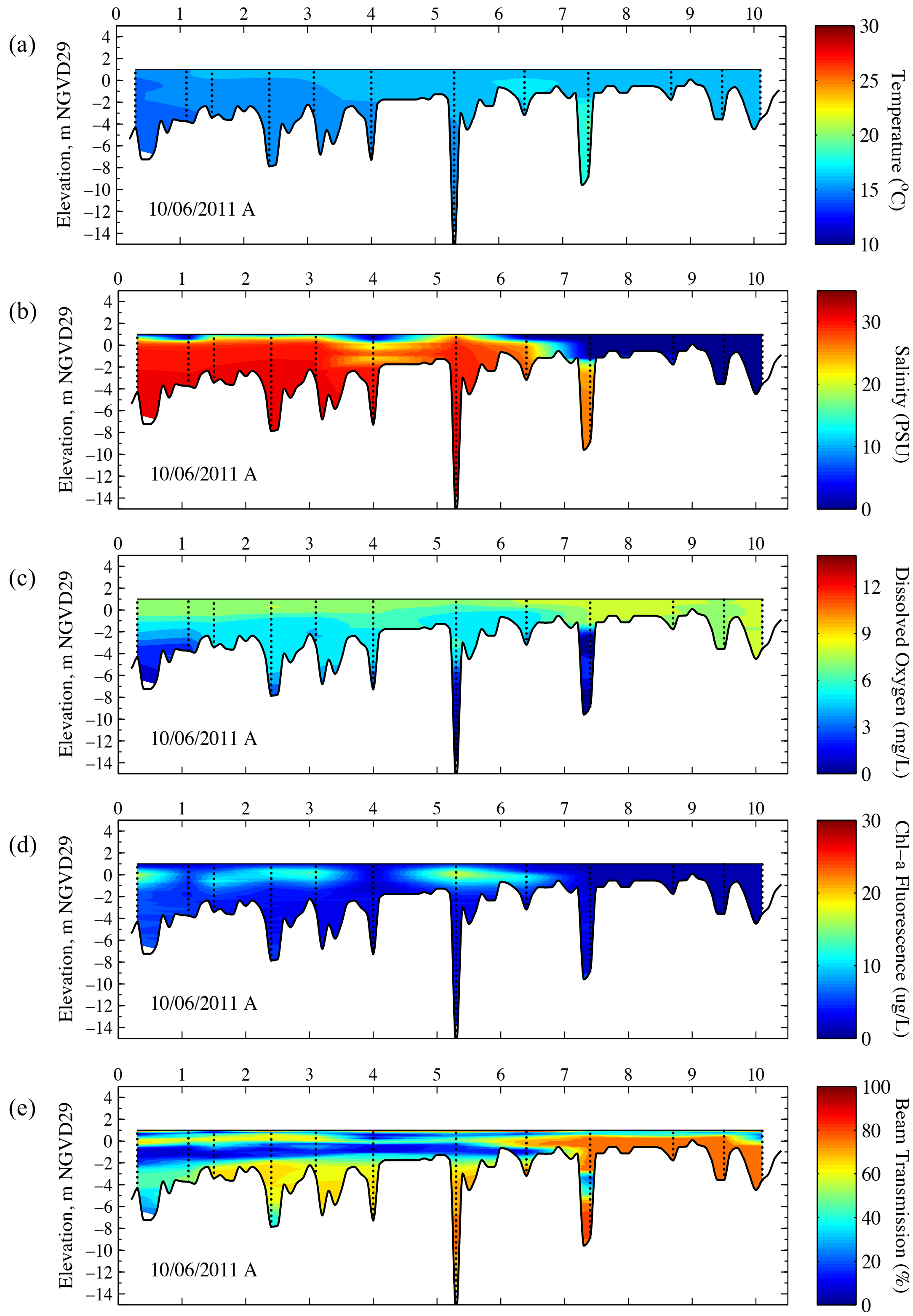

Figure 9.11 Contours of temperature (a), salinity (b), dissolved oxygen (c), chlorophyll fluorescence (d), and beam transmission (e) collected on 6 October 2011. The x-axis represents distance (in km) from the estuary mouth.

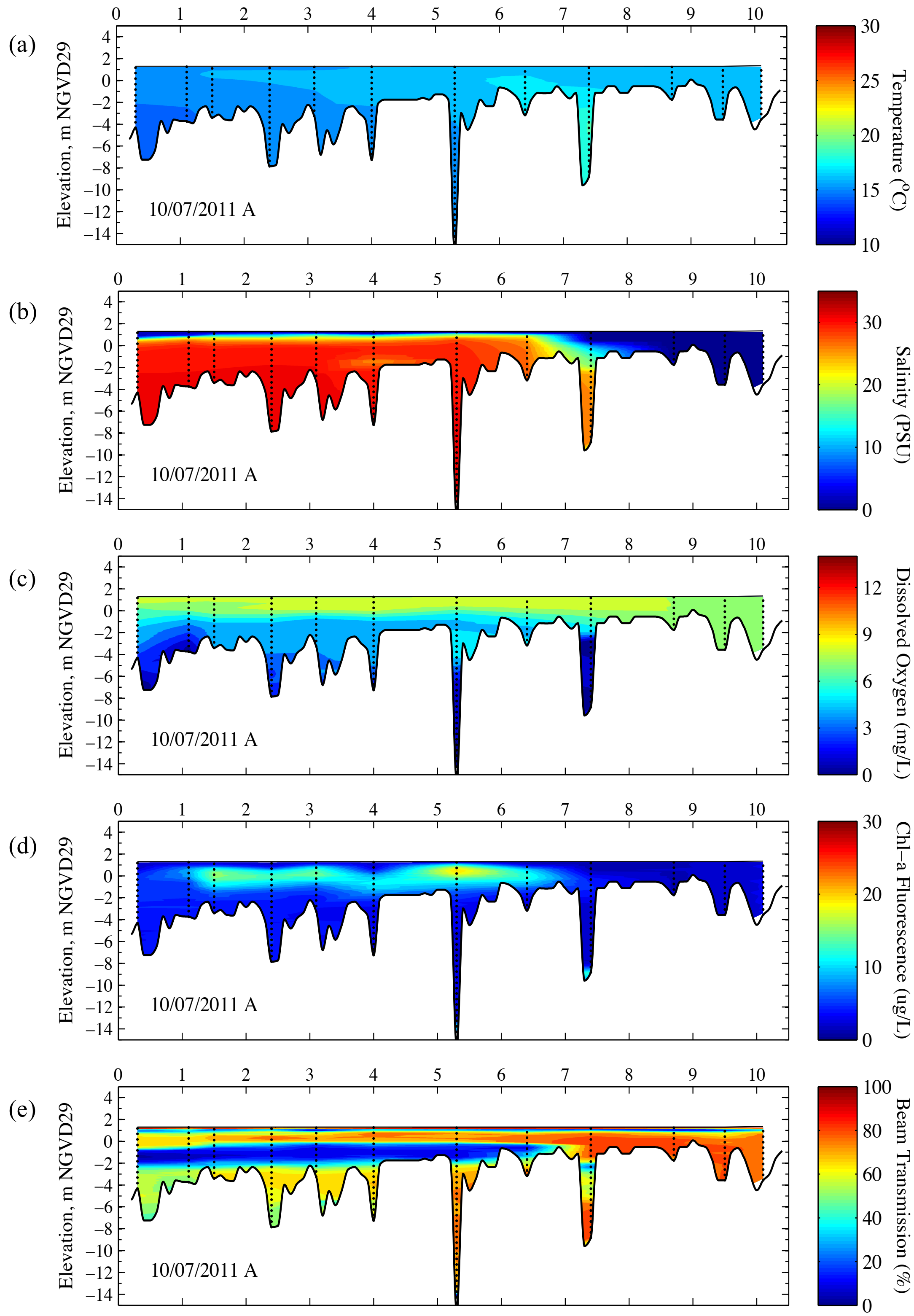

Figure 9.12 Contours of temperature (a), salinity (b), dissolved oxygen (c), chlorophyll fluorescence (d), and beam transmission (e) collected on 7 October 2011. The x-axis represents distance (in km) from the estuary mouth.

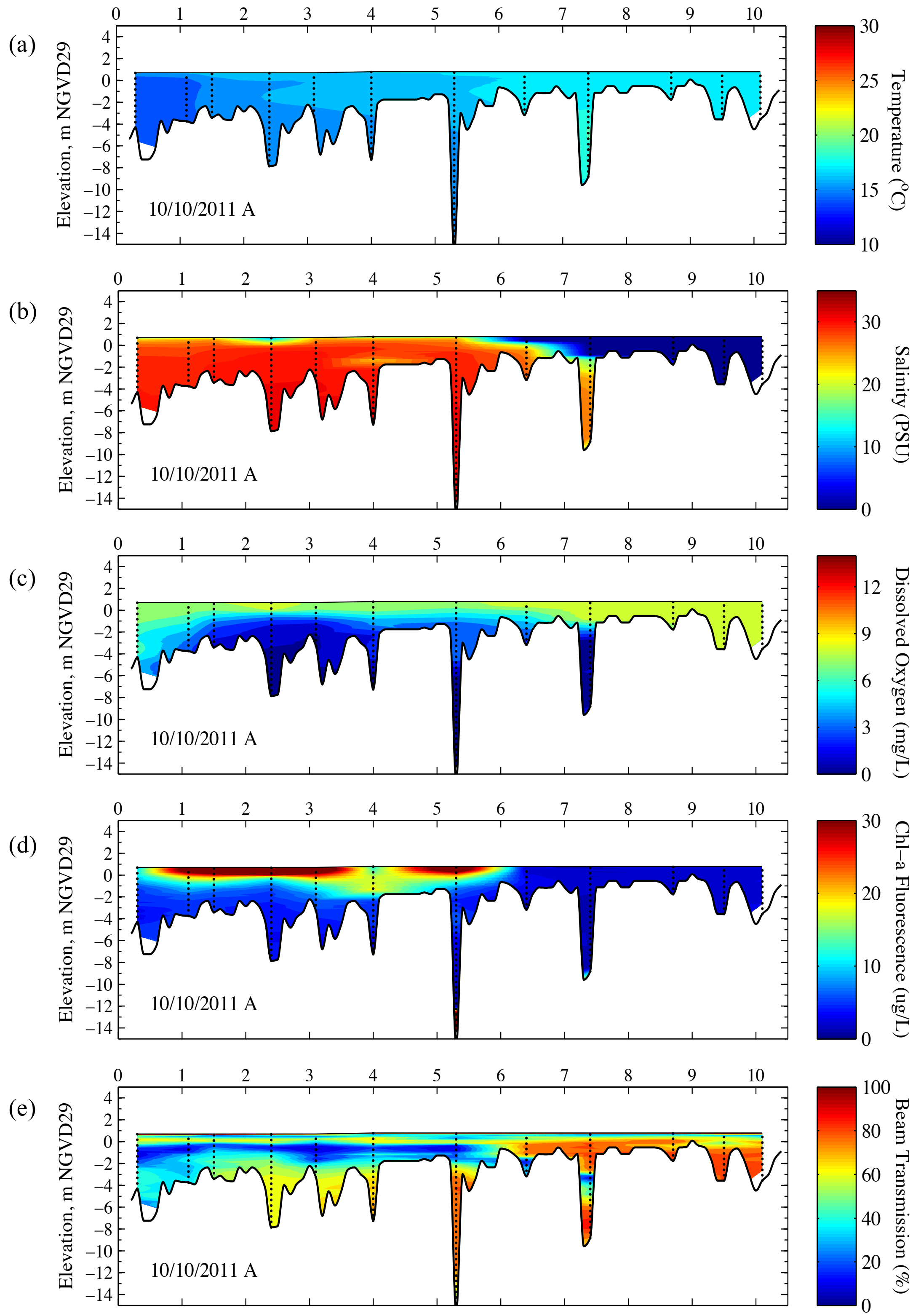

Figure 9.13 Contours of temperature (a), salinity (b), dissolved oxygen (c), chlorophyll fluorescence (d), and beam transmission (e) collected on 10 October 2011. The x-axis represents distance (in km) from the estuary mouth.

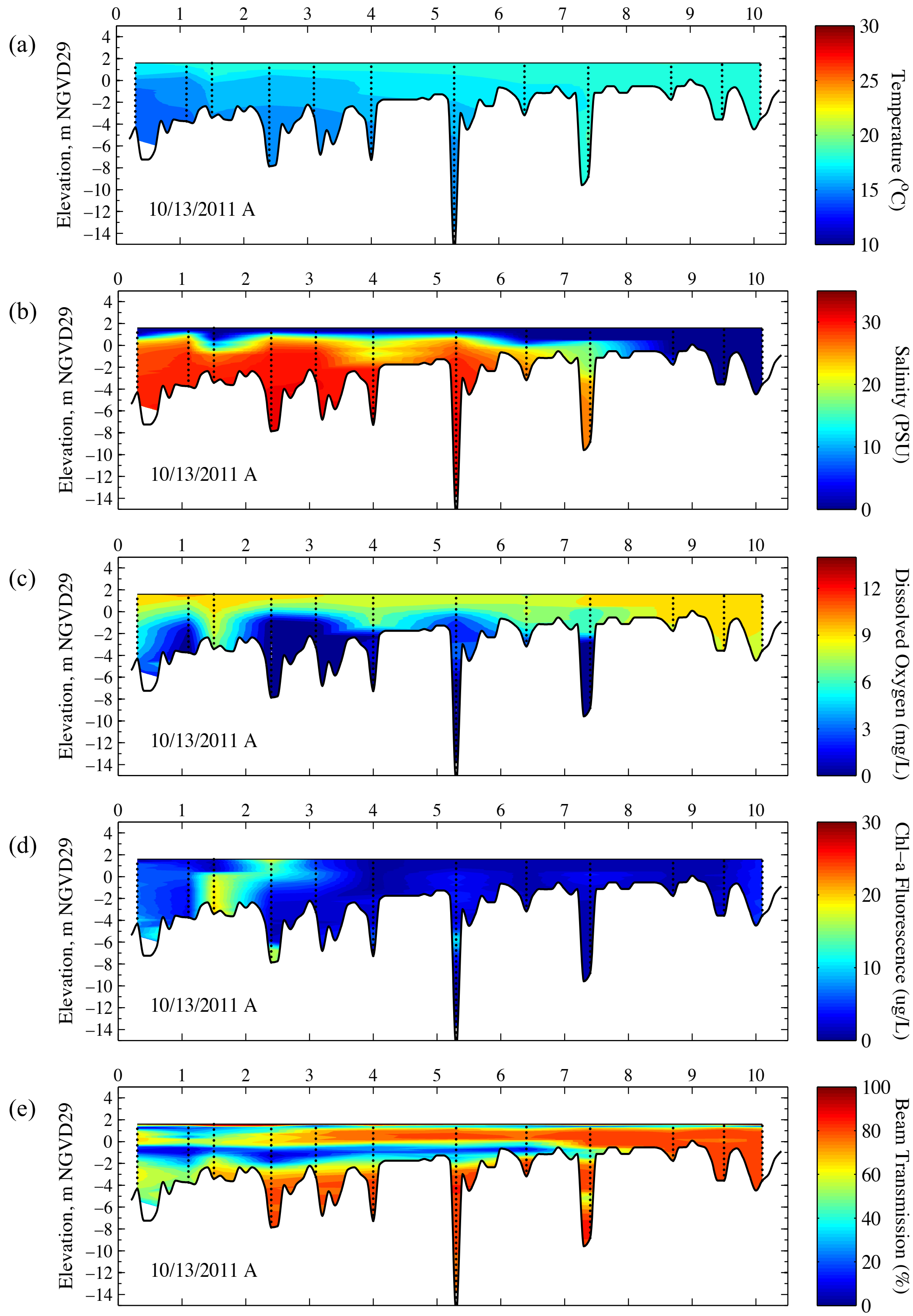

Figure 9.14 Contours of temperature (a), salinity (b), dissolved oxygen (c), chlorophyll fluorescence (d), and beam transmission (e) collected on 13 October 2011. The x-axis represents distance (in km) from the estuary mouth.

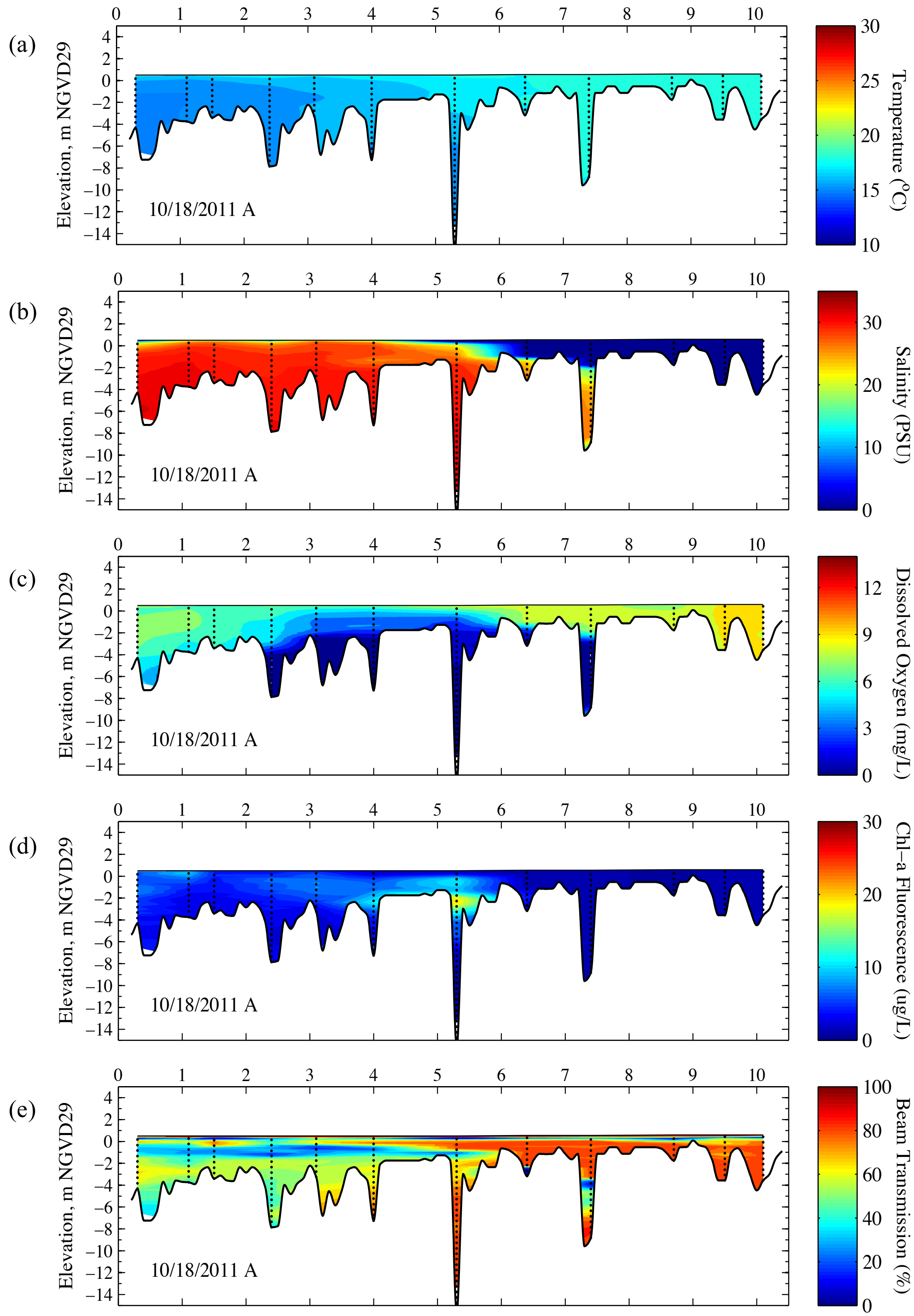

Figure 9.15 Contours of temperature (a), salinity (b), dissolved oxygen (c), chlorophyll fluorescence (d), and beam transmission (e) collected on 18 October 2011. The x-axis represents distance (in km) from the estuary mouth.

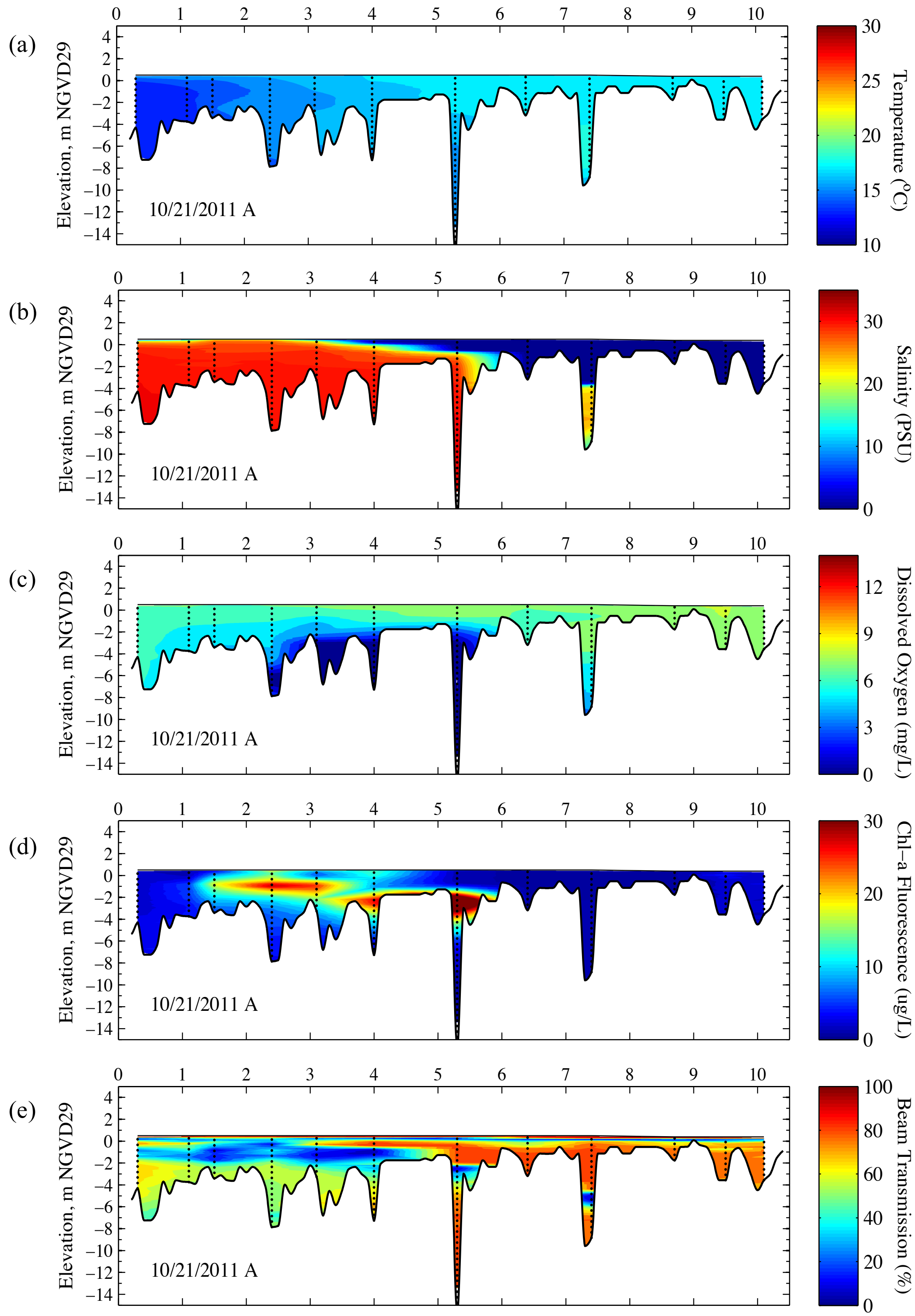

Figure 9.16 Contours of temperature (a), salinity (b), dissolved oxygen (c), chlorophyll fluorescence (d), and beam transmission (e) collected on 21 October 2011. The x-axis represents distance (in km) from the estuary mouth.

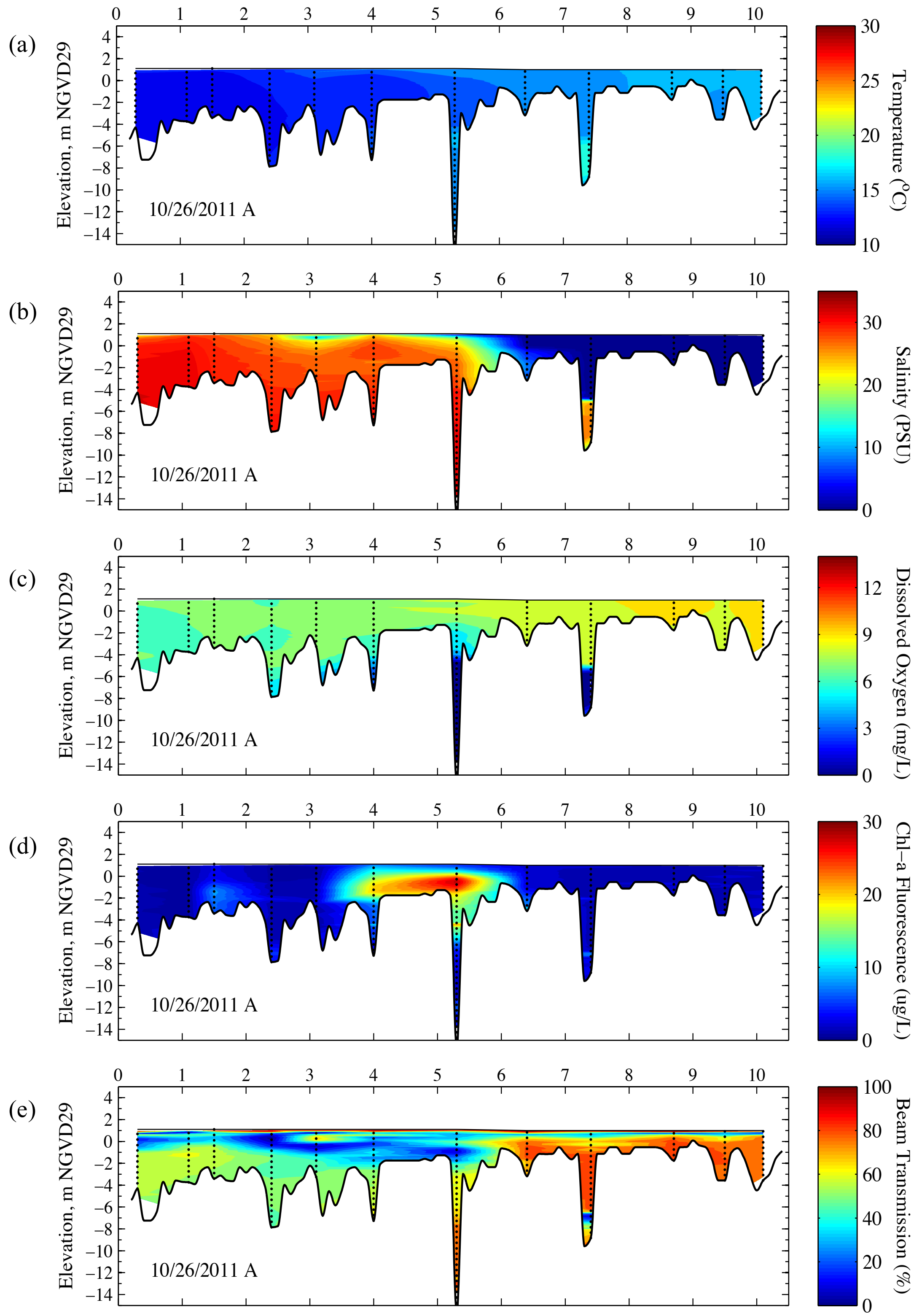

Figure 9.17 Contours of temperature (a), salinity (b), dissolved oxygen (c), chlorophyll fluorescence (d), and beam transmission (e) collected on 26 October 2011. The x-axis represents distance (in km) from the estuary mouth.

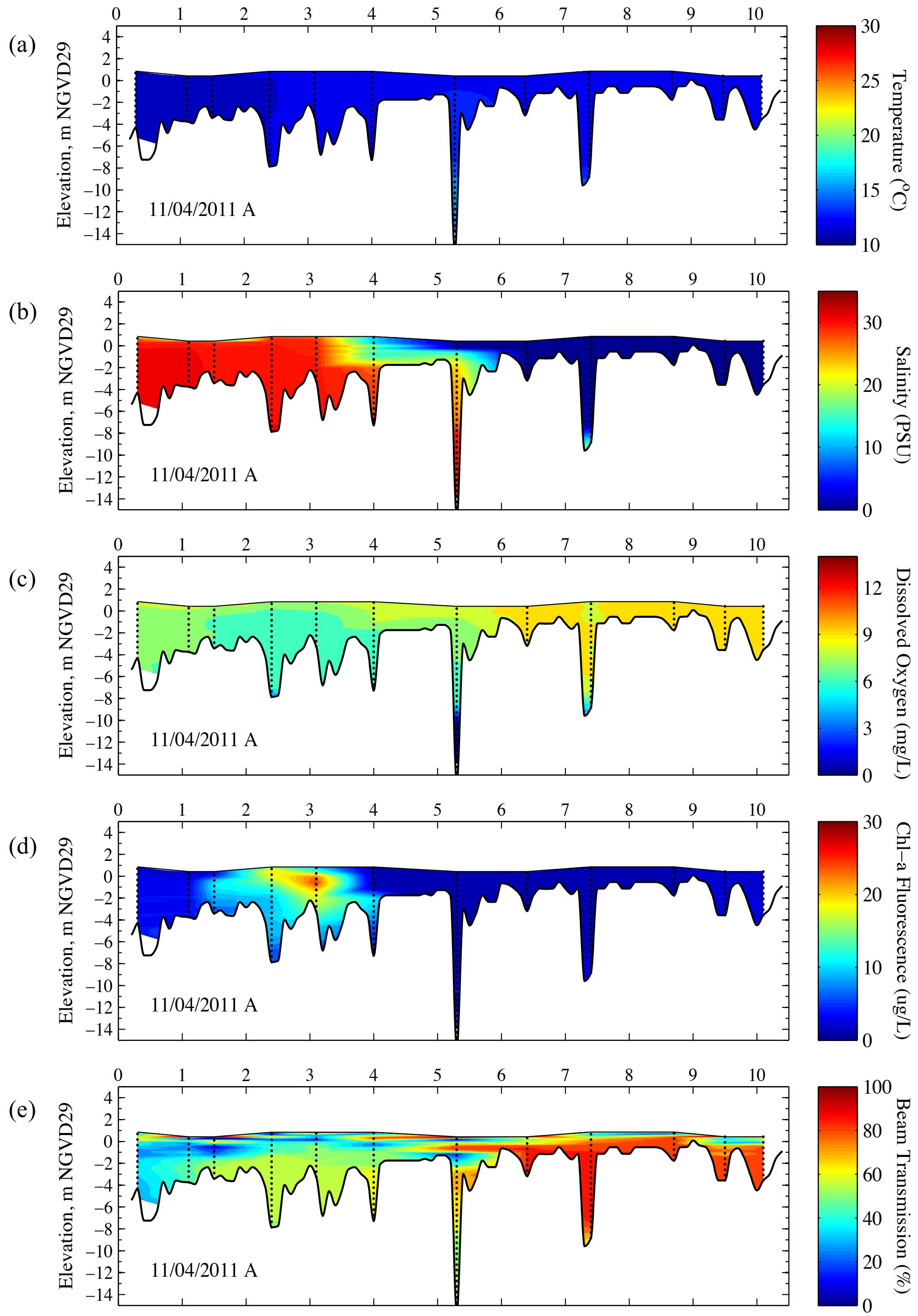

Figure 9.18 Contours of temperature (a), salinity (b), dissolved oxygen (c), chlorophyll fluorescence (d), and beam transmission (e) collected on 4 November 2011. The x-axis represents distance (in km) from the estuary mouth.

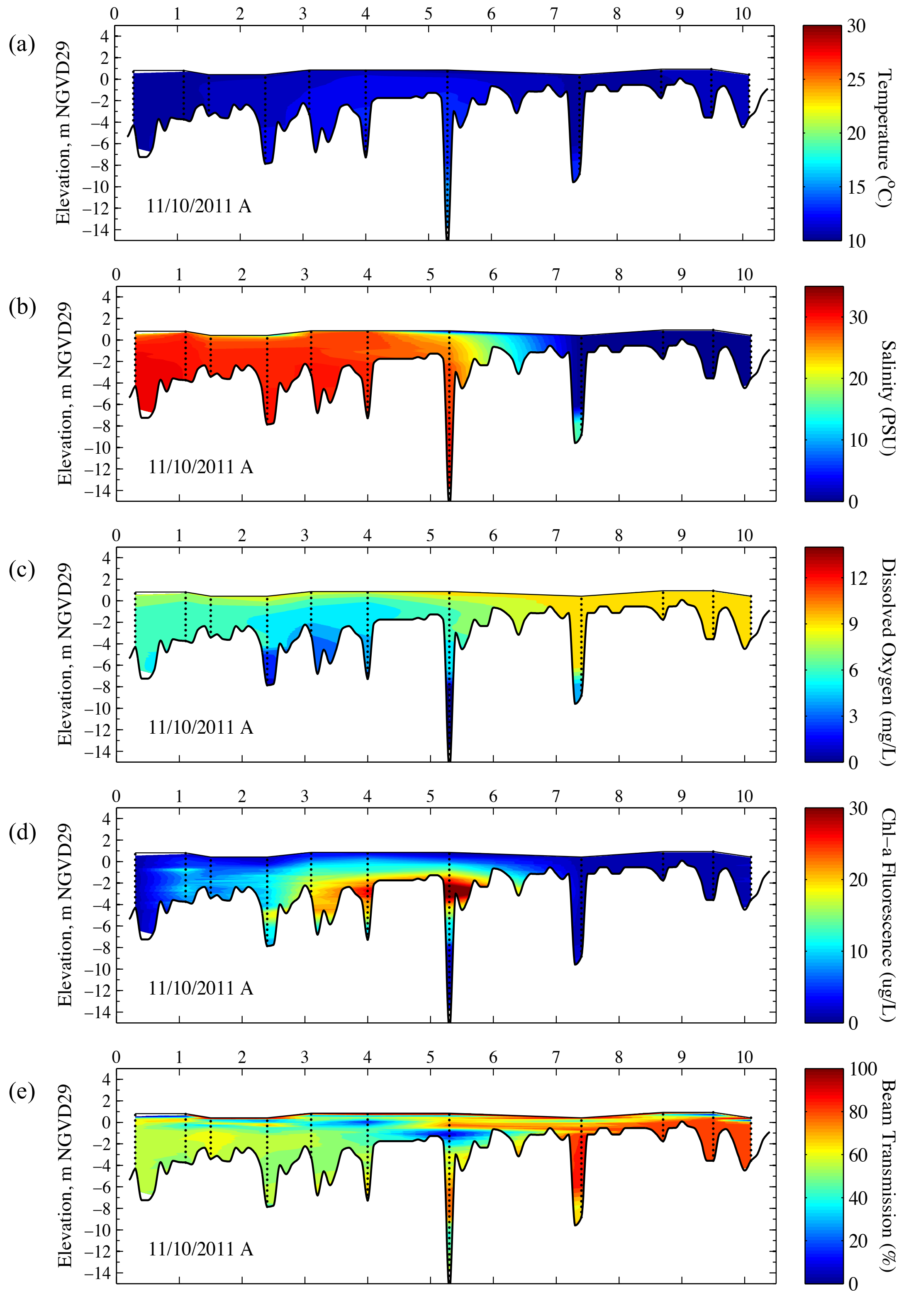

Figure 9.19 Contours of temperature (a), salinity (b), dissolved oxygen (c), chlorophyll fluorescence (d), and beam transmission (e) collected during the first transect on 10 November 2011. The x-axis represents distance (in km) from the estuary mouth.

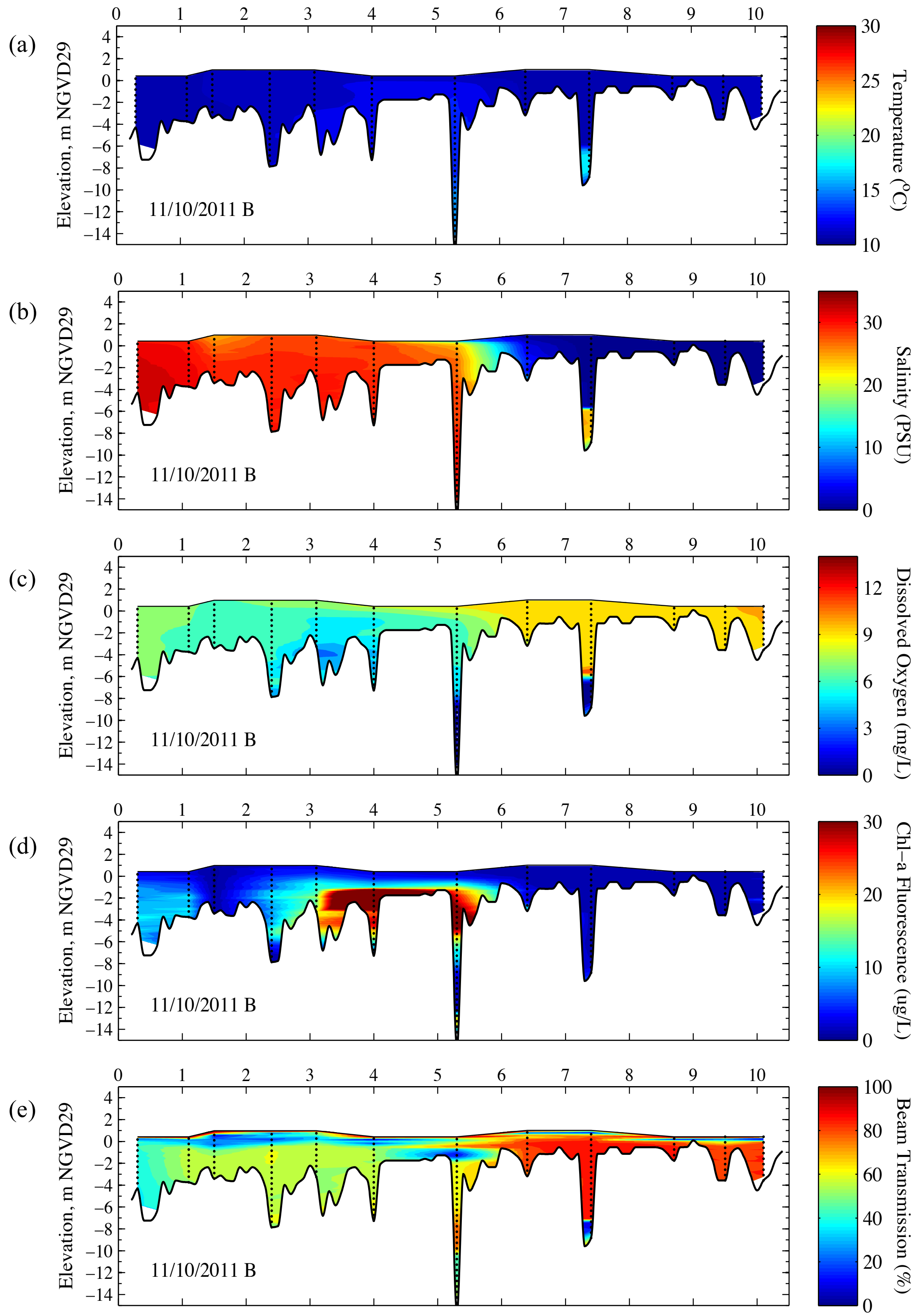

Figure 9.20 Contours of temperature (a), salinity (b), dissolved oxygen (c), chlorophyll fluorescence (d), and beam transmission (e) collected during the second transect on 10 November 2011. The x-axis represents distance (in km) from the estuary mouth.

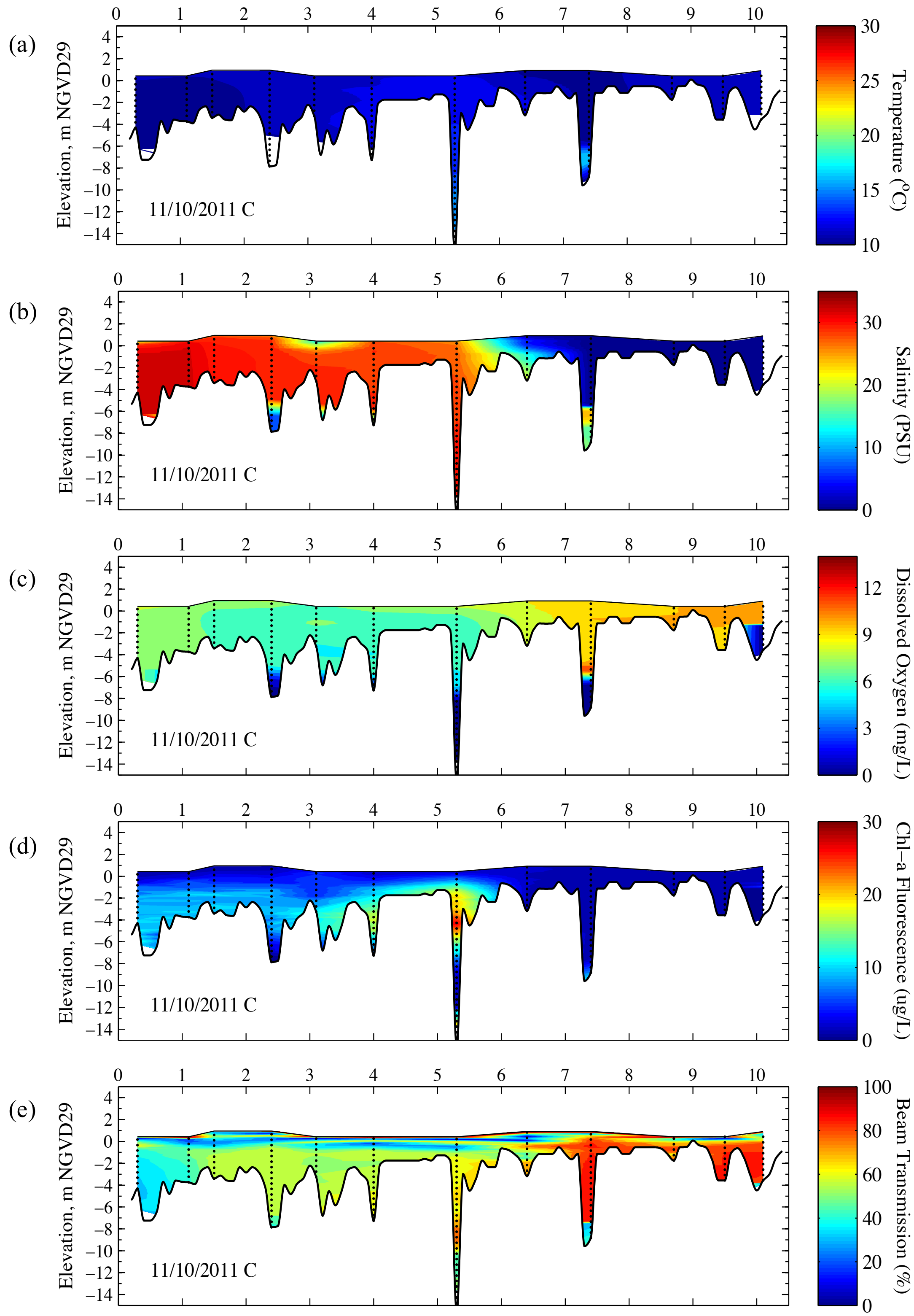

Figure 9.21 Contours of temperature (a), salinity (b), dissolved oxygen (c), chlorophyll fluorescence (d), and beam transmission (e) collected during the third transect on 10 November 2011. The x-axis represents distance (in km) from the estuary mouth.

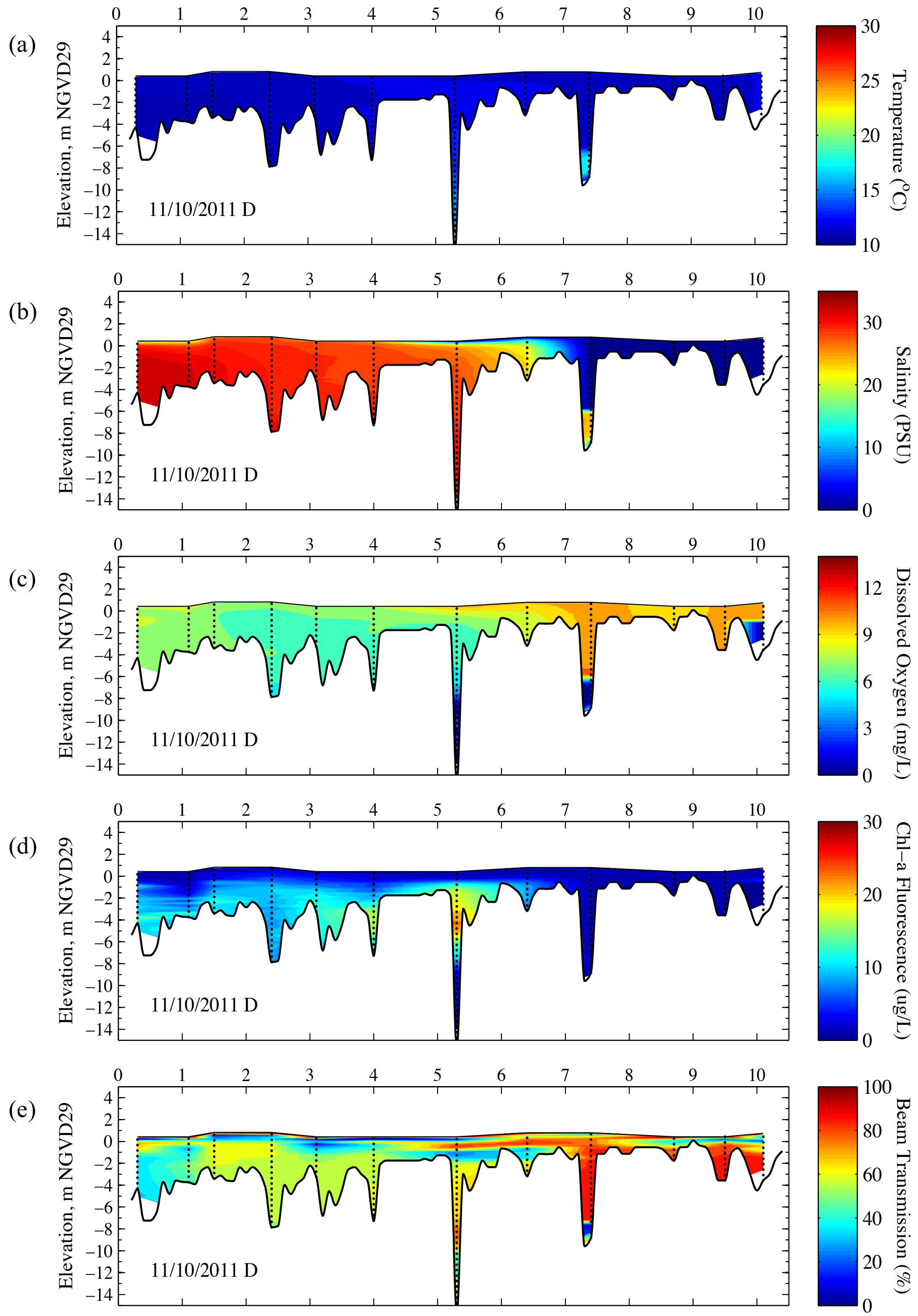

Figure 9.22 Contours of temperature (a), salinity (b), dissolved oxygen (c), chlorophyll fluorescence (d), and beam transmission (e) collected during the fourth transect on 10 November 2011. The x-axis represents distance (in km) from the estuary mouth.

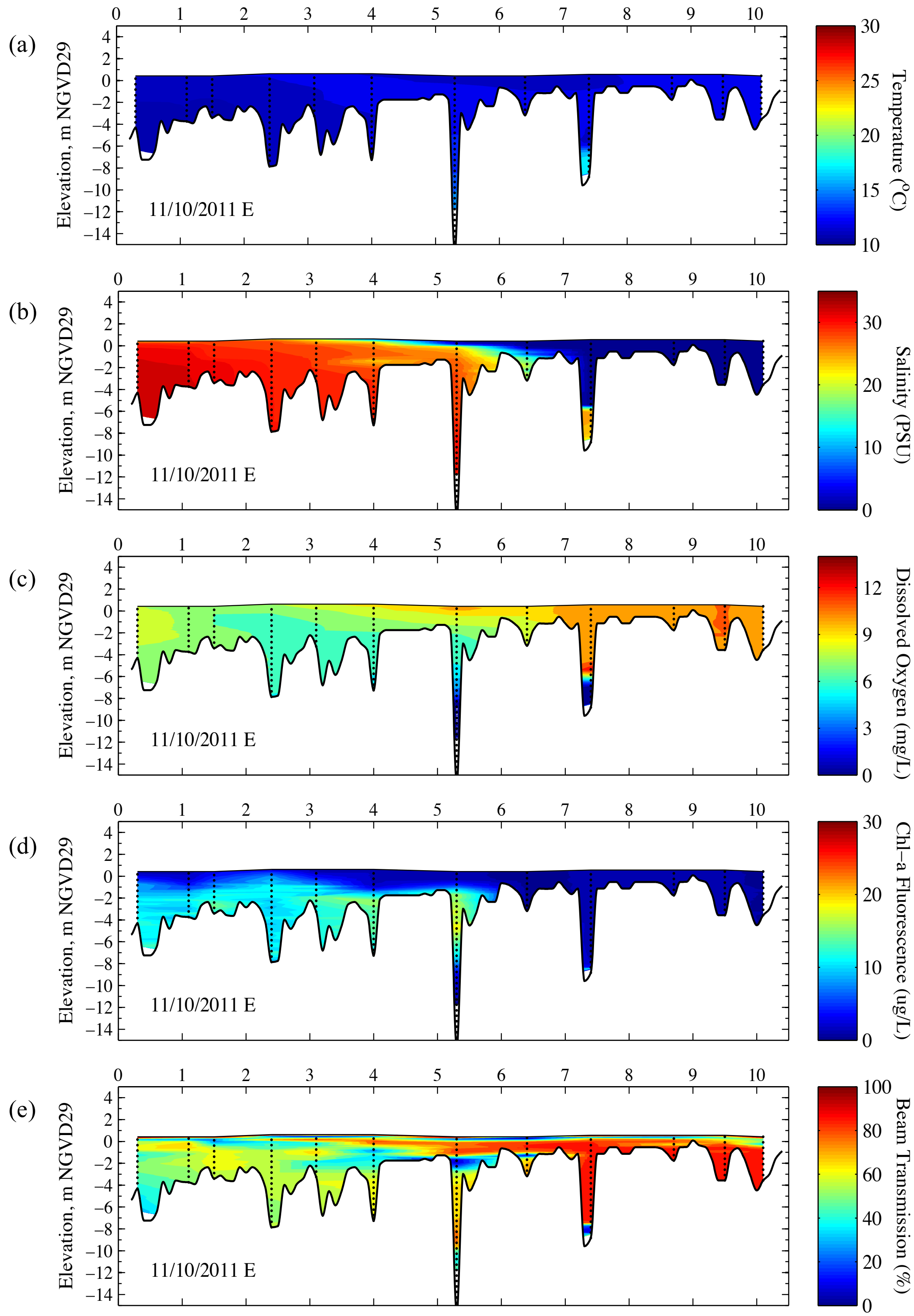

Figure 9.23 Contours of temperature (a), salinity (b), dissolved oxygen (c), chlorophyll fluorescence (d), and beam transmission (e) collected during the fifth transect on 10 November 2011. The x-axis represents distance (in km) from the estuary mouth.